Soil horizon C was sampled after digging 30∿50cm depth and removing humus(horizon A) and horizon B. The sample was then dried in air at the site and 100g of under 80 mesh was taken for analysis.

During the work of the previous year, Ag, Cu, Pb, Zn were used as the indicator elements. From the results, Cu and Zn geochemical anomalies were confirmed to show the old mines and mineralized zones very clearly. Also Pb anomalies were detected in this area. Thus for the present work, Cu, Pb, Zn were used as the indicators. Atomic absorption was used with the precedure shown in the flow chart of Fig. 7.

2-2 Processing and Interpretation of Data

The analytical data (Table 1) were processed and studied as shown in the flow chart of Fig. 8 and the anomalies and anomalous zones were extracted.

The total number of samples collected during this work is 635. The area of 2.3 km E-W and 1.0 km N-S was first delineated for the detailed investigation and 450 samples were collected from here. After processing and studying the analytical data, it was recognized that the anomalous zone extended southward. Thus 185 more samples were collected from the above extension of the anomalous zone. The statistical analysis of the analytical data, however, were carried out on the original 450 samples, because many of the additional samples showed anomalous values and they were excluded.

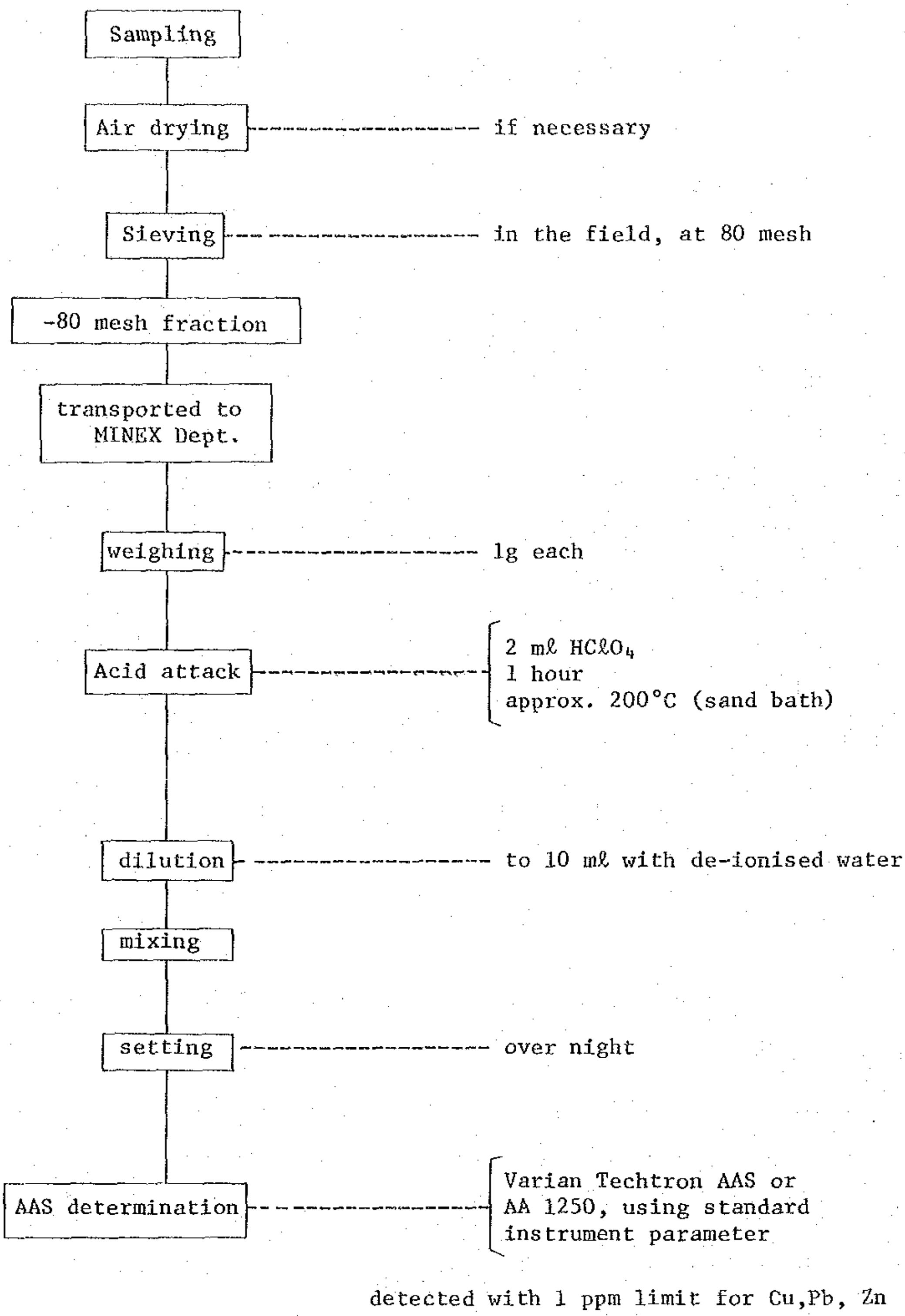

Fig. 7 Flow chart for Pretreatment and Geochemical Analysis of the Soil Samples

Table I The Results of Geochemical Analysis of Soil Samples in Kamiyobo Area

Sample No.	Cu ppm	Pb ppm	Zn ppm	Sample No.	Cu ppm	Pb ppm	Zn ppm	Sample No.	Cu ppm	Pb ppm	Zn ppm	Sample No.	Cu ppm	Pb ppm	Zn ppm	Sample No.	Cu ppm	Pb ppm	Zn ppm
A-1	40	40	30	B-1	32	40	24	C-1	22	40	20	D-1	20	38	40	E-1	20	38	32
2	32	28	28	2	46	50	33	2	36	48	25	2	24	42	40	2	20	40	30
3	20	18	18	3	40	38	30	3	38	44	27	3	30	56	50	3	36	54	50
4	20	18	23	4	34	26	22	4	42	36	26	4	48	64	68	4	70	80	80
5	18	16	20	5	30	20	21	5	48	30	30	5	56	58	81	5	140	180	120
6	24	20	25	6	26	16	21	6	36	22	20	6	60	52	90	6	78	60	140
7	22	20	26	7	24	20	18	7	24	20	20	7	60	36	60	7	100	50	100
8	18	18	25	8	22	20	19	8	28	20	20	8	34	24	40	8	42	24	32
9	18	16	24	9	16	18	15	9	28	18	16	9	30	22	35	9	40	14	18
10	16	18	32	10	20	18	17	10	22	24	24	10	40	20	45	10	6	14	18
11	10	12	18	11	18	16	16	11	30	24	22	11	38	26	82	11	8	16	20
12	10	14	16	12	30	20	22	12	22	22	40	12	22	30	76	12	10	18	32
13	14	14	34	13	12	16	21	13	14	24	40	13	10	20	51	13	10	18	44
14	90	18	50	14	30	20	31	14	10	18	26	14	10	24	53	14	10	20	44
15	46	22	60	15	44	22	24	15	12	20	33	15	10	22	40	15	30	22	54
16	38	24	90	16	16	24	40	16	18	24	80	16	10	26	54	16	70	24	80
17	40	22	91	17	38	18	25	17	16	20	43	17	14	24	52	17	22	20	40
18	40	22	92	18	80	20	25	18	18	18	30	18	14	24	62	18	20	24	50
19	30	28	100	19	44	18	40	19	12	14	20	19	10	18	55	19	14	20	58
20	12	14	44	20	18	14	35	20	10	12	16	20	10	20	41	20	14	18	28
21	14	14	41	21	12	10	21	21	10	10	12	21	10	16	25	21	12	16	20
22	16	14	40	22	12	12	20	22	22	12	10	22	12	22	32	22	16	18	24
23	16	16	32	23	14	22	15	23	16	16	14	23	14	24	30	23	20	26	26
24	14	14	25	24	14	18	15	24	14	14	12	24	15	24	26	24	38	44	40
25	16	16	20	25	18	16	16	25	18	18	16	25	20	30	32	25	50	58	54
26	18	16	16	26	22	14	13	26	22	20	19	26	22	34	35	26	60	60	60
27	20	20	21	27	20	18	15	27	22	20	18	27	44	58	60	27	52	60	60
28	20	20	18	28	24	20	18	28	28	24	20	28	60	76	70	28	54	56	50
29	22	22	17	29	26	20	21	29	40	32	43	29	58	66	70	29	56	50	42
30	28	22	20	30	30	22	18	30	32	38	16	30	70	72	75	30	70	48	50
31	28	22	20	31	34	28	19	31	54	56	30	31	70	64	80	31	60	42	48
32	24	20	15	32	42	34	20	32	60	58	31	32	44	66	54	32	58	38	42
33	34	28	20	33	46	38	20	33	54	58	29	33	66	58	70	33	52	28	40
34	24	24	16	34	50	40	30	34	66	60	40	34	62	60	64	34	60	38	40
35	30	30	25	35	56	40	24	35	80	68	40	35	50	46	60	35	40	24	30
36	22	28	15	36	58	44	40	36	78	60	36	36	50	50	60	36	58	30	40
37	30	28	20	37	52	44	30	37	58	44	40	37	50	44	59	37	50	26	30
38	28	28	17	38	44	40	25	38	52	40	25	38	44	38	55	38	38	20	28
39	30	30	21	39	46	38	26	39	50	40	24	39	42	38	50	39	32	20	24
40	30	28	20	40	54	40	27	40	44	38	20	40	40	34	50	40	32	18	20
41	32	30	20	41	52	38	25	41	42	38	25	41	42	30	43	41	34	20	22
42	36	32	21	42	60	40	30	42	50	32	23	42	38	30	46	42	30	22	40
43	32	32	18	43	56	40	25	43	52	36	23	43	50	32	43	43	54	26	38
44	36	34	24	44	42	36	26	44	42	30	17	44	40	30	50	44	38	20	26
45	38	34	24	45	46	32	28	45	34	24	20	45	50	28	50	45	44	24	30

- Continue -

Sample No.	Cu ppm	Pb ppm	Zn ppm	Sample No.	Cu ppm	Pb ppm	Zn ppm	Sample No.	Cu ppm	Pb ppm	Zn ppm	Sample No.	Cu ppm	Pb ppm	Zn ppm	Sample No.	Cu ppm	Pb ppm	Zn ppm
F-1	18	22	41	G-1	22	28	31	H-1	16	16	28	I-1	14	20	33	J-1	8	16	20
2	22	50	41	2	30	38	38	2	40	30	52	2	32	40	64	2	30	32	63
3	34	42	58	3	56	40	58	3	120	48	160	3	20	28	44	3	22	36	51
4	64	62	98	4	120	140	360	4	160	94	400	4	40	40	70	4	26	38	63
5	76	78	200	5	100	120	300	5	160	100	410	5	95	70	240	5	50	52	93
6	100	88	300	6	100	180	400	6	160	100	500	6	100	120	500	6	74	80	250
7	92	60	220	7	100	200	600	7	120	120	540	7	120	180	500	7	120	100	400
8	100	38	160	8	140	120	400	8	140	100	700	8	100	160	600	8	160	220	700
9	95	30	79	9	140	64	350	9	220	160	800	9	120	260	700	9	180	320	600
10	44	16	36	10	130	60	300	10	180	120	400	10	180	200	550	10	120	400	420
11	40	12	42	11	90	20	45	11	160	100	180	11	140	220	410	11	100	300	300
12	50	14	50	12	74	14	43	12	100	32	100	12	140	200	380	12	140	300	400
13	26	10	32	13	40	16	42	13	58	30	61	13	140	180	300	13	140	380	400
14	14	10	27	14	22	10	20	14	40	24	58	14	120	180	310	14	120	200	410
15	22	12	42	15	32	10	24	15	50	36	52	15	100	160	240	15	140	200	400
16	16	10	48	16	22	14	20	16	58	50	60	16	100	160	310	16	160	120	250
17	16	10	43	17	20	16	21	17	62	70	78	17	120	220	300	17	100	60	92
18	22	12	39	18	30	20	28	18	120	140	230	18	100	140	240	18	76	38	74
19	23	14	37	19	52	40	40	19	60	70	80	19	90	70	82	19	42	20	46
20	20	12	32	20	52	64	61	20	54	54	63	20	50	32	40	20	22	16	30
21	26	20	39	21	60	66	62	21	42	38	49	21	30	20	31	21	24	16	34
22	38	36	50	22	62	64	60	22	32	26	38	22	28	18	27	22	24	14	35
23	62	58	75	23	56	50	52	23	100	32	61	23	28	16	26	23	18	10	26
24	58	50	70	24	52	44	43	24	30	20	34	24	24	16	25	24	20	10	29
25	56	46	63	25	50	38	41	25	20	18	26	25	24	12	20	25	16	10	23
26	48	34	54	26	40	32	35	26	26	18	29	26	22	14	22	26	18	12	25
27	54	34	60	27	46	28	30	27	24	16	30	27	28	14	24	27	16	10	26
28	46	30	46	28	36	22	25	28	22	18	28	28	24	10	22	28	18	10	24
29	44	20	43	29	36	20	28	29	28	16	30	29	26	12	24	29	24	11	32
30	40	20	40	30	38	20	34	30	30	12	30	30	32	14	32	30	32	12	33
31	40	18	35	31	50	22	35	31	30	15	31	31	34	14	30	31	40	16	42
32	38	16	38	32	40	16	30	32	30	12	30	32	52	22	40	32	44	18	45
33	42	16	34	33	50	20	30	33	46	18	42	33	42	20	33	33	66	22	56
34	38	12	33	34	46	18	32	34	54	20	46	34	44	20	34	34	40	18	44
35	50	16	37	35	60	20	37	35	54	20	61	35	74	26	53	35	100	38	200
36	52	20	39	36	64	22	40	36	42	16	51	36	60	20	39	36	200	60	320
37	62	20	41	37	80	24	44	37	95	30	85	37	120	60	300	37	70	30	83
38	68	22	40	38	78	28	61	38	200	100	600	38	26	12	20	38	24	14	30
39	54	24	42	39	88	32	64	39	48	38	85	39	100	60	310	39	28	20	48
40	62	20	50	40	60	30	53	40	12	14	30	40	12	12	18	40	34	26	74
41	46	20	40	41	50	22	46	41	10	10	25	41	12	14	20	41	26	22	94
42	50	18	40	42	36	16	31	42	12	10	20	42	14	16	20	42	34	26	77
43	48	18	35	43	32	16	33	43	22	18	33	43	12	18	20	43	20	18	31
44	40	20	30	44	30	14	25	44	16	14	26	44	18	20	29	44	20	18	36
45	40	18	35	45	22	12	20	45	14	14	20	45	22	22	31	45	22	20	41

- Continue -

Sample No.	Cu ppm	Pb ppm	Zn ppm	Sample No.	Cu ppm	Pb ppm	Zn ppm	Sample No.	Cu ppm	Pb ppm	Zn ppm	Sample No.	Cu ppm	Pb ppm	Zn ppm	Sample No.	Cu ppm	Pb ppm	Zn ppm
K-1	3	6	5	L-1	4	10	8	M-1	3	7	7	N-1	3	6	5	O-1	2	6	3
2	8	12	14	2	6	11	10	2	4	6	5	2	2	6	5	2	2	6	3
3	14	22	28	3	15	17	25	3	8	10	10	3	2	5	4	3	2	6	4
4	12	26	26	4	24	30	40	4	16	16	22	4	4	7	7	4	2	7	3
5	11	25	28	5	12	16	20	5	21	30	32	5	9	10	12	5	2	4	2
6	16	38	60	6	22	36	50	6	34	46	70	6	22	21	38	6	2	5	3
7	30	62	100	7	50	100	160	7	26	40	100	7	160	100	100	7	6	8	10
8	62	100	150	8	40	100	200	8	120	120	320	8	150	280	360	8	18	12	34
9	140	320	300	9	38	98	200	9	110	250	460	9	76	120	300	9	22	12	58
10	130	220	300	10	70	260	300	10	84	100	300	10	56	100	220	10	56	23	54
11	100	130	260	11	86	180	200	11	80	180	580	11	88	180	280	11	20	10	20
12	100	140	400	12	120	100	220	12	180	240	500	12	72	48	100	12	14	8	18
13	160	100	540	13	200	60	230	13	72	60	200	13	50	34	64	13	15	6	16
14	200	36	120	14	140	30	105	14	82	36	110	14	70	50	96	14	16	5	8
15	84	20	36	15	120	38	130	15	180	100	340	15	66	52	100	15	18	6	8
16	86	28	62	16	74	44	100	16	140	52	100	16	54	20	42	16	24	8	11
17	42	24	32	17	36	20	36	17	64	28	50	17	40	13	20	17	30	7	12
18	26	16	18	18	20	10	16	18	42	15	26	18	32	10	22	18	21	6	13
19	18	12	12	19	13	6	8	19	32	10	24	19	20	10	22	19	20	7	22
20	15	11	10	20	12	6	9	20	20	8	18	20	50	16	68	20	25	10	40
21	12	10	9	21	10	5	10	21	20	9	19	21	130	18	80	21	58	12	66
22	11	10	8	22	9	5	8	22	28	11	26	22	88	20	82	22	92	12	52
23	22	10	20	23	24	11	21	23	21	10	18	23	32	12	27	23	52	12	42
24	20	10	20	24	24	10	20	24	22	10	20	24	26	11	28	24	26	10	28
25	20	9	16	25	16	8	16	25	10	8	14	25	16	8	18	25	8	8	13
26	15	8	13	26	18	10	18	26	27	10	18	26	20	8	14	26	20	10	19
27	15	8	12	27	32	10	22	27	24	10	16	27	20	8	11	27	54	17	58
28	22	10	20	28	24	10	18	28	56	14	36	28	60	15	30	28	44	16	40
29	40	14	26	29	50	17	38	29	68	22	56	29	84	34	100	29	34	12	25
30	42	14	32	30	38	16	38	30	50	20	52	30	68	17	46	30	23	10	22
31	54	17	44	31	64	26	60	31	62	18	56	31	84	14	50	31	44	12	38
32	43	20	44	32	62	34	65	32	92	22	80	32	62	14	34	32	20	9	16
33	64	32	64	33	40	40	82	33	80	26	82	33	62	12	34	33	19	10	13
34	100	33	82	34	160	90	300	34	170	23	100	34	22	11	32	34	20	10	18
35	110	44	100	35	140	66	200	35	180	24	140	35	36	13	32	35	36	13	32
36	160	70	180	36	58	26	62	36	32	13	32	36	36	12	26	36	36	12	26
37	44	28	60	37	40	14	25	37	22	12	26	37	15	10	16	37	15	10	16

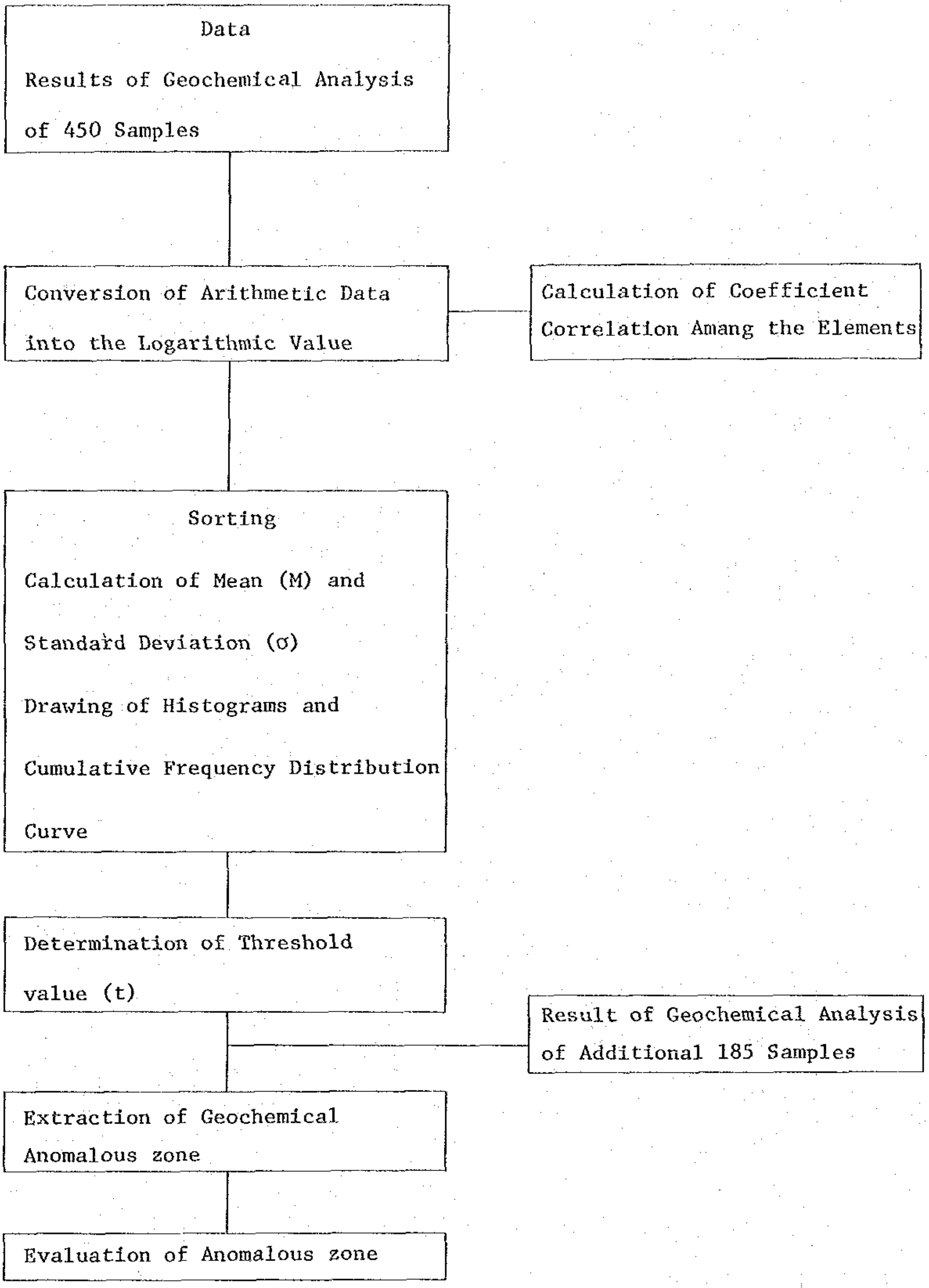

Fig. 8 Flow Chart of Statistical Treatment of Geochemical Data

More than 60 percent of the samples were collected from localities with no exposures. Also as the distribution of the intrusive and carbonate rocks is very narrow and thus the amount of samples from these localities is less than 10 percent. Therefore, the 450 data were processed without classification.

The analytical values were all converted into logarithmic values, and histogram and cumulative frequency distribution curves were prepared (Figs. 9, 10).

The behavior of each component is close to lognormal distribution as shown in Figs. 9, 10. The mean value (M) and the standard deviation (σ) is as follows.

Element	Mean (M)	$\log$ Standard deviation(σ)
Cu	37	.303627
Pb	29	.317458
Zn	45	.382264
Pb + Zn	77	.344227
Cu + Pb + Zn	117	.320779

The correlation of the components is as follows.

Element	Coefficient of Correlation
Cu —— Pb	.76
Pb —— Zn	.80
Zn —— Cu	.74
Zn —— Pb+Zn	.97
Zn —— Cu+Pb+Zn	.98
Pb+Zn —— Cu+Pb+Zn	.95

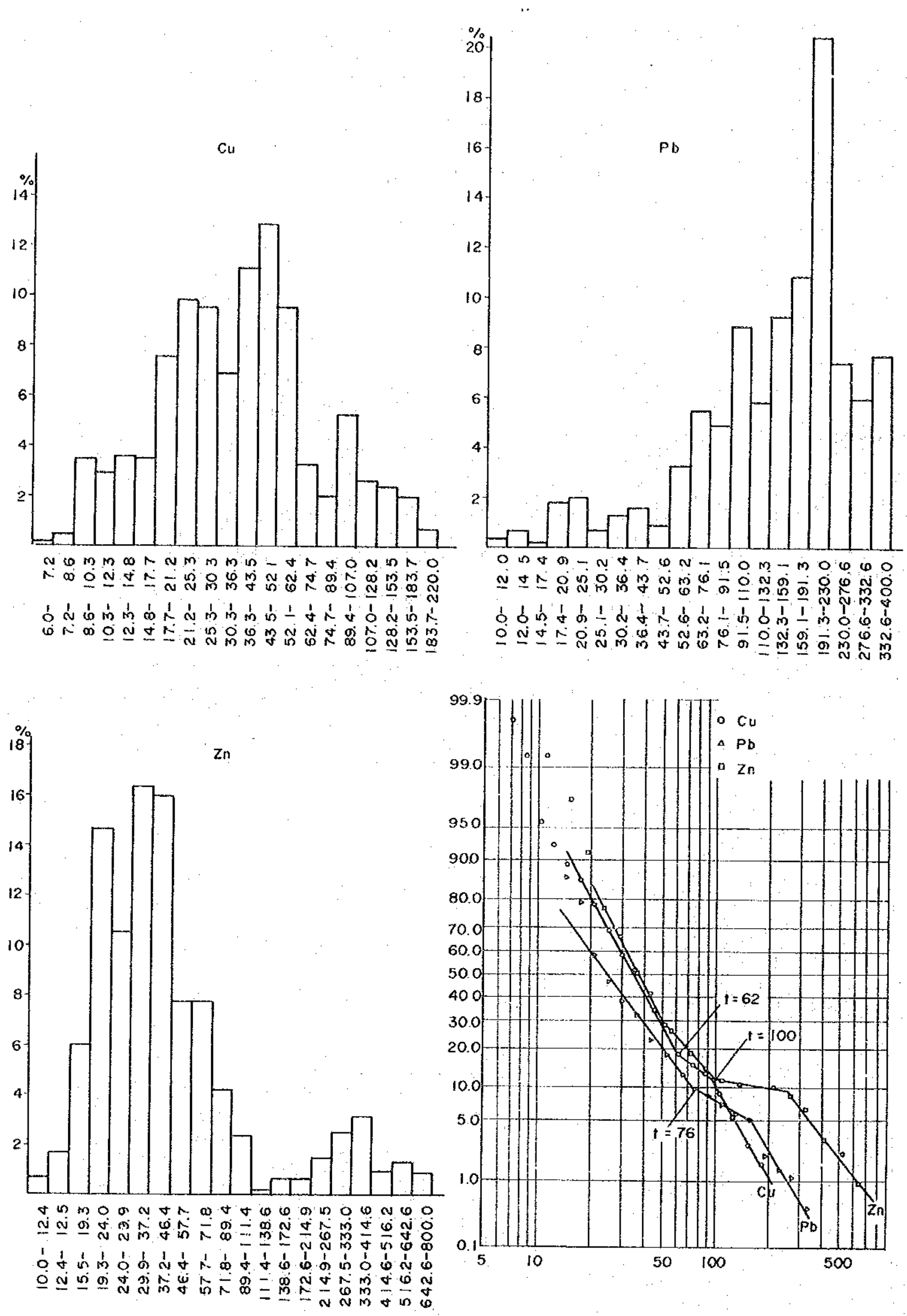

Fig. 9 Histogram and Cumulative Frequency Distribution Curve of Geochemical Date (Cu, Pb, Zn)

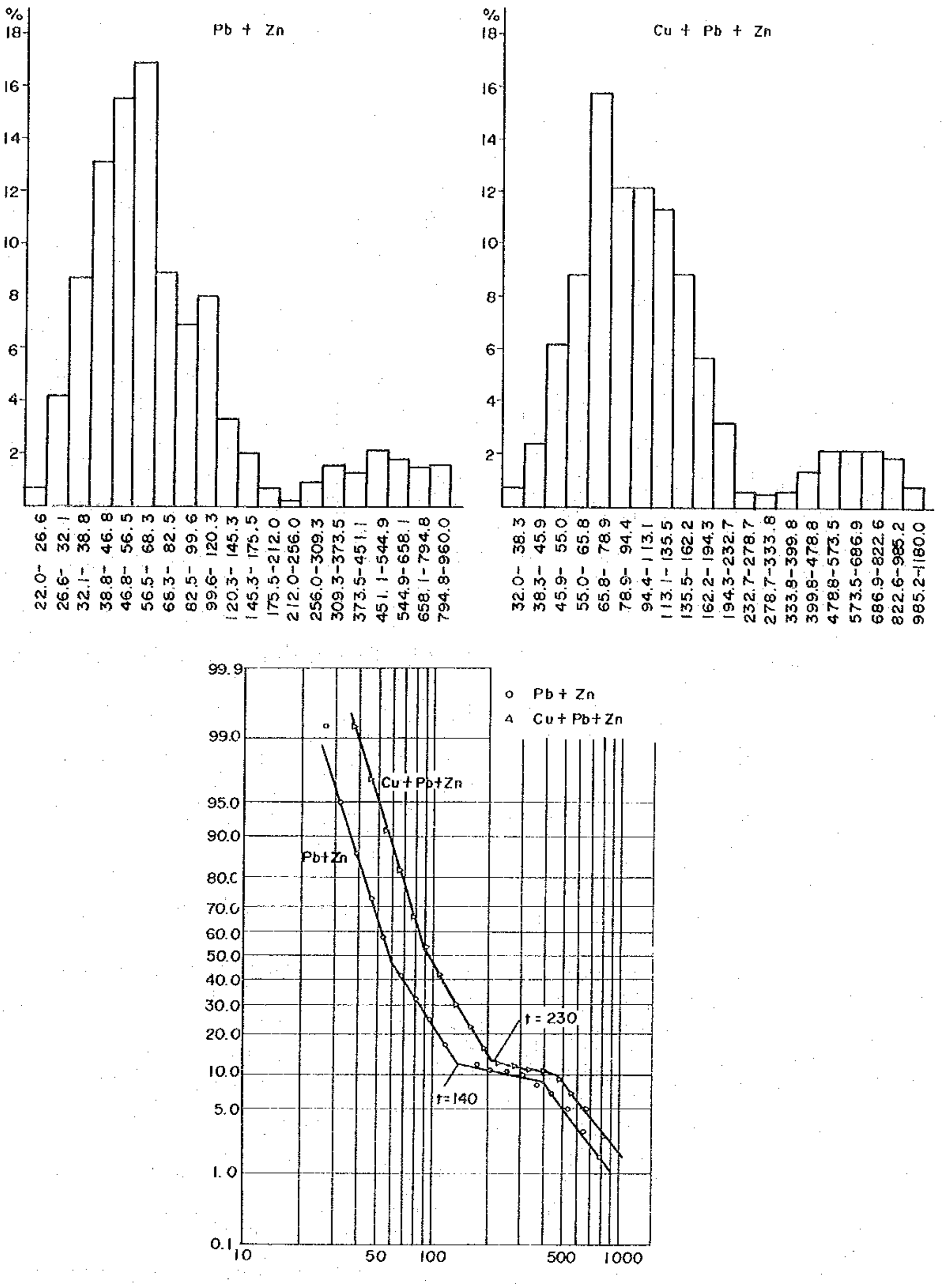

Fig. 10 Histogram and Cumulative Frequency Distribution Curve of Combined Geochemical Date

The M+σ, M+2σ, M+3σ and the threshold values (t) obtained from the cumulative frequency distribution are as follows.

Element	M +σ	M+2σ	M+3σ	t
Cu	74 ppm	149 ppm	299 ppm	62 ppm
Pb	61	126	262	76
Zn	108	260	628	100
Pb + Zn	169	373	825	130
Cu+Pb+Zn	244	510	1,068	230

Geochemical anomaly maps using the above values were prepared. Similar anomalous zones were extracted by using M+σ and t values, but with M+2σ, the shape of the anomalous zones obtained was not continuous. Therefore, as in the previous year, we used the threshold values for determining the anomalous values. Also M+2σ and M+3σ were used as supplementary figures for clarifying the centers of the anomalous zones.

2-3 Extraction of Anomalous Zones and Evaluation

The anomalous zones extracted by using the anomalous values determined by the method described above is shown in Figs. 11,12. It is clearly seen from these maps that the anomalous zones of each component coincide very well. The only notable differences are that there are scattered independent small Cu anomalies and that the Pb anomalies tend to be discontinous in the southeast. At the central part of the anomalous zone, there is no M+3σ zone for Cu, and those

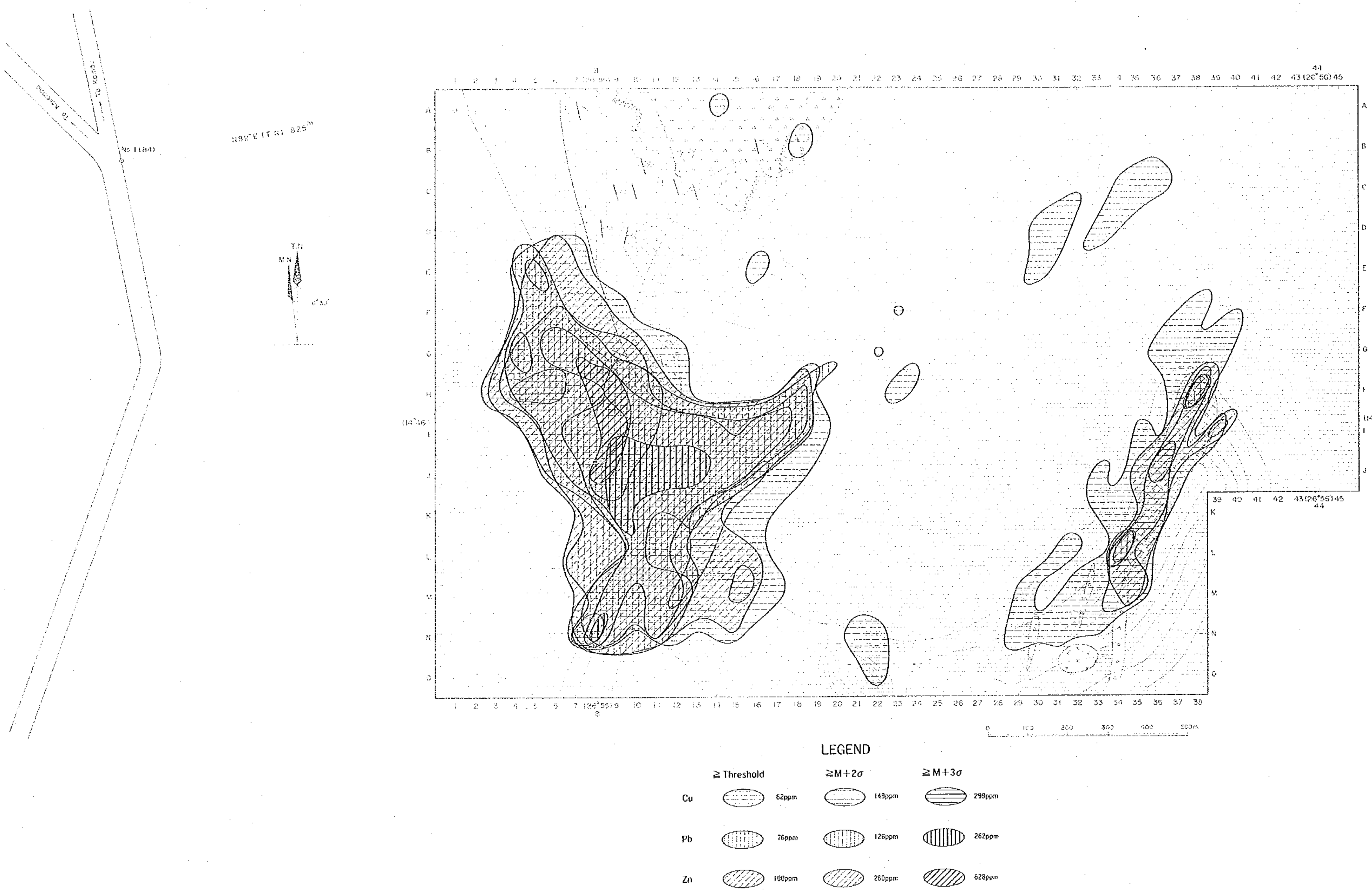

Fig. 11 Map of Geochemical Anomalous Zones in Kamiyobo Area (Cu, Pb, Zn)

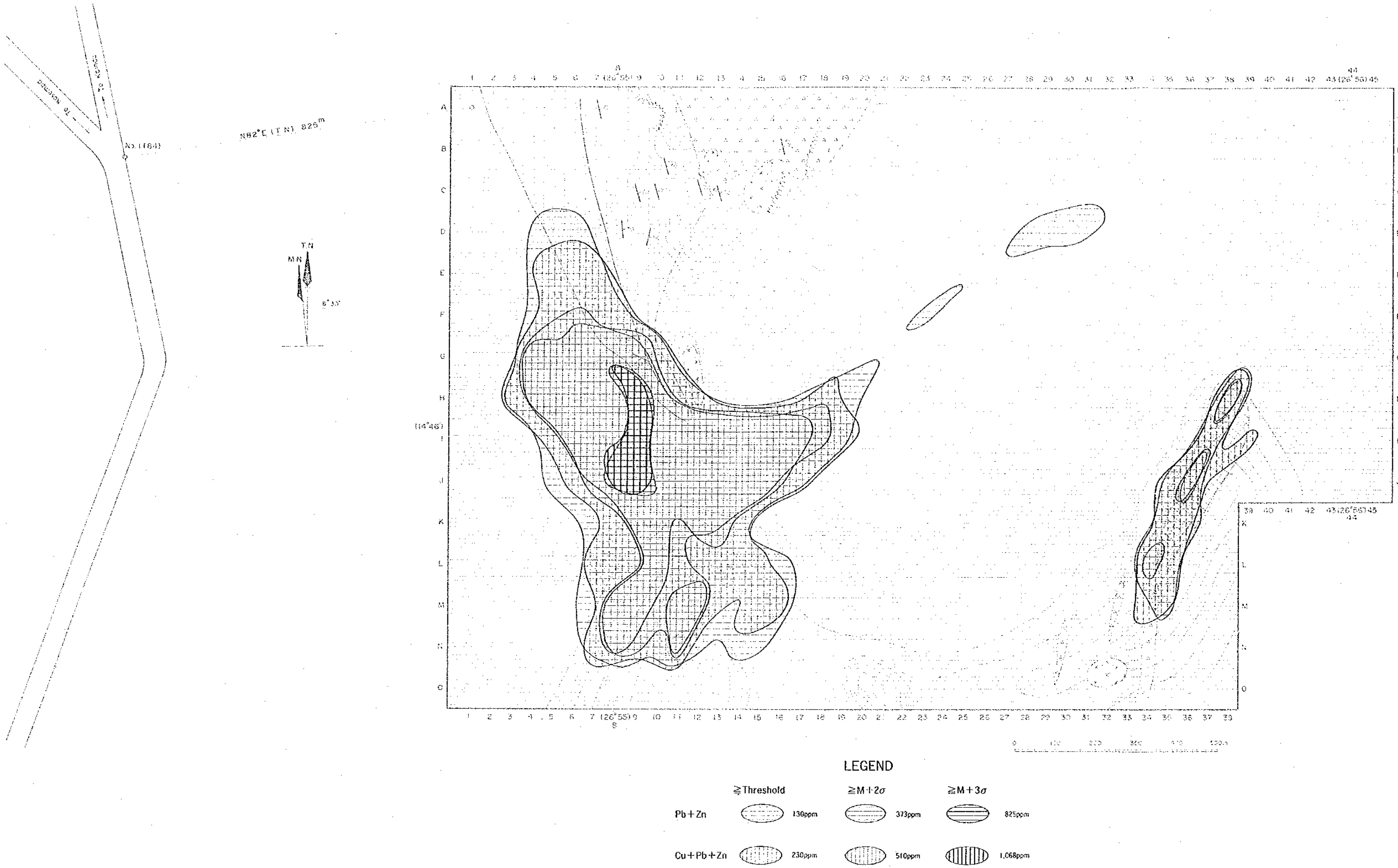

Fig. 12 Map of Geochemical Anomalous Zones in Kamiyobo Area (Cu+Pb, Cu+Pb+Zn)

for Pb and Zn do not coincide accurately. The anomalous zones of Pb + Zn and Cu + Pb + Zn were prepared by smoothening the relatively small individual differences. There is very little difference between these two zones. The only difference is that Pb+Zn zones have somewhat clearer direction of elongation, and as the development of lead and zinc resources are of higher priority at present, we will evaluate the Pb+Zn anomalous zones.

The Pb+Zn geochemical anomalous zones were found to occur relatively widely in the southwest and in vein-form in the southeastern part of this area. The zone in the southwest consists of two peaks for each traverse (Fig. 13), and two directions of elongation NNW-SSE and NE-SW can be determined by connecting these peaks. On the other hand, the vein-type zone in southeast is elongated in NNE-SSW direction. Of these anomalous zones, the southwestern NNW-SSE zone has the highest anomaly, and contains the largest number of values higher than $M+3\sigma$.

Pb+Zn mineralization cannot be observed as outcrops in the anomalous zones because the exposure is extremely poor in this area. The NNW-SSE trending anomalous zones are elongated in the direction harmoniously with the boundary between the bedded limestone and metasediments. The NE-SW trending zones are more or less parallel to the topographic ridge of the area. The NNE-SSW trending zones are elongated along the boundary of hematite-magnetite exposure which is mentioned in section 1-2.

The evaluation of the geochemical results based on above considerations are summarized in Table 2.

Table 2 The List of Geochemical Anomalous Zones

Anomalous Zone	Amounts of over Critical Value(t)		Maximum Value (ppm)	Extention of Anomalous Zone(m)		Rock	* Evaluation
	Element	≥t		High Anomalous Zone (≧M+3σ)	Whole Zone (≥ t)		
South West NNW-SSE Anomalous Zone	Cu		220	-	1,100	Meta Sedi-ments	A
	Pb		400	250	1,000		
	Zn		800	300	1,050		
	Pb + Zn		960	300	1,150		
	Cu+Pb+Zn		1,180	300	1,050		
South West NE-SW Anomalous Zone	Cu		200	-	900	Meta Sedi-ments	B
	Pb		380	100	950		
	Zn		540	-	900		
	Pb + Zn		780	-	1,000		
	Cu+Pb+Zn		800	-	900		
South West NNW-SSE + NE-SW Anomalous Zone	Cu	91					
	Pb	64					
	Zn	85					
	Pb + Zn	96					
	Cu+Pb+Zn	82					
South East NNE-SSW Anomalous Zone	Cu	33	200	-	900	Meta Sedi-ments	B
	Pb	2	100	-	100		
	Zn	11	600	-	650		
	Pb + Zn	9	700	-	650		
	Cu+Pb+Zn	11	900	-	650		

* A : Progressive prospections necessary

B : To be studied after result of A

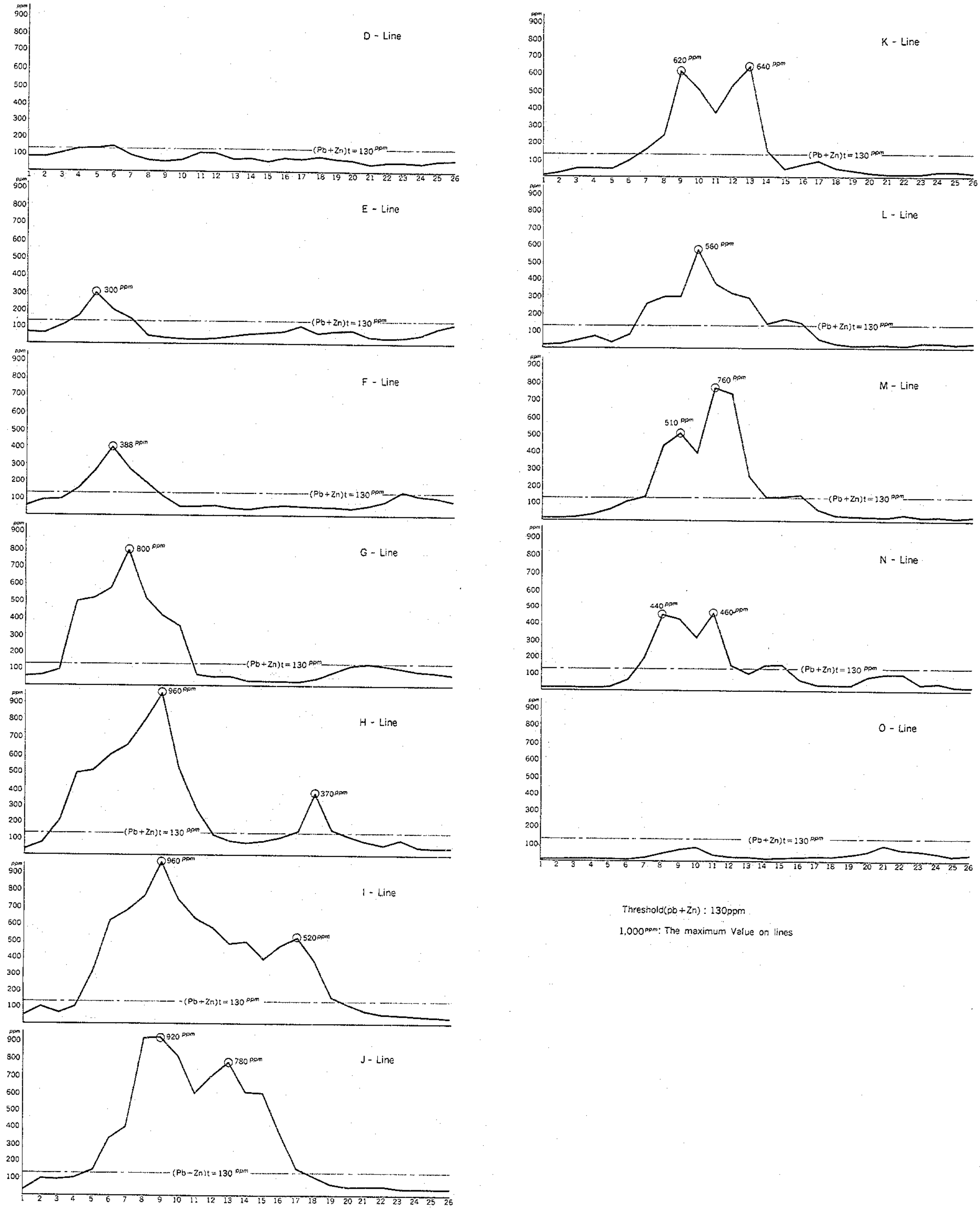

Fig. 13 Characteristic Curve of Geochemical Value in Anomalous Zones of Kamiyobo Area

Chapter 2 Sable Antelope Area (Geophysical Prospecting)

1. Introduction

Measurements of induced polarization (IP) are made either in the frequency-domain or the time-domain method. In this field survey, the frequency-domain measurements have been conducted in which the frequency effect is obtained by apparent resistivities measured at two different frequencies.

In spectral induced polarization (SIP) method, one measures the magnitude and phase lag of IP response at a broad range of frequencies. The SIP method contains more data than in a case of IP method, and a frequency spectrum of IP response will be helpful in discrimination of different metallic minerals or in eliminating electromagnetic coupling.

1-1 The Purpose of the Survey

The measurements of controlled source audiofrequency magnetotellurics (CSAMT) at the first year have delineated the most promising area along a tectonic line which passes in the vicinities of Sable Antelope and Blue Jacket. The area has been recommended as a target of detailed investigation.

In the second year, the IP and SIP methods are carried out over this area to detect anomalous fields, to elucidate their character, and to delineate an extent of mineralized zone and its continuity to a depth.

1-2 The Surveyed Area

The surveyed area by the IP and SIP methods is of some 2 sq.km and covers an abandoned mine named Sable Antelope. a mineralized zone called Blue Jacket and zones of low apparent resistivity which were detected by the CSAMT method in the first year (Fig. 14).

1-3 Field Parameters

Field parameters were set as follows:

(1) IP method

Electrode Configuration:	dipole-dipole array
Electrode Separation:	100m
Electrode Separation Index:	n=1 to 5
Frequencies:	0.125 & 1.0 Hz(2 frequencies)

Line Lengths : Five lines totalling 16km

Line A	4km
Line B	4km
Line C	4km
Line D	2km
Line E	2km

(2) SIP method

Electrode Configuration:	dipole-dipole array
Electrode Separation:	100m
Electrode Separation Index:	n=1 to 5
Frequencies:	0.125 to 88 Hz (18 frequencies)

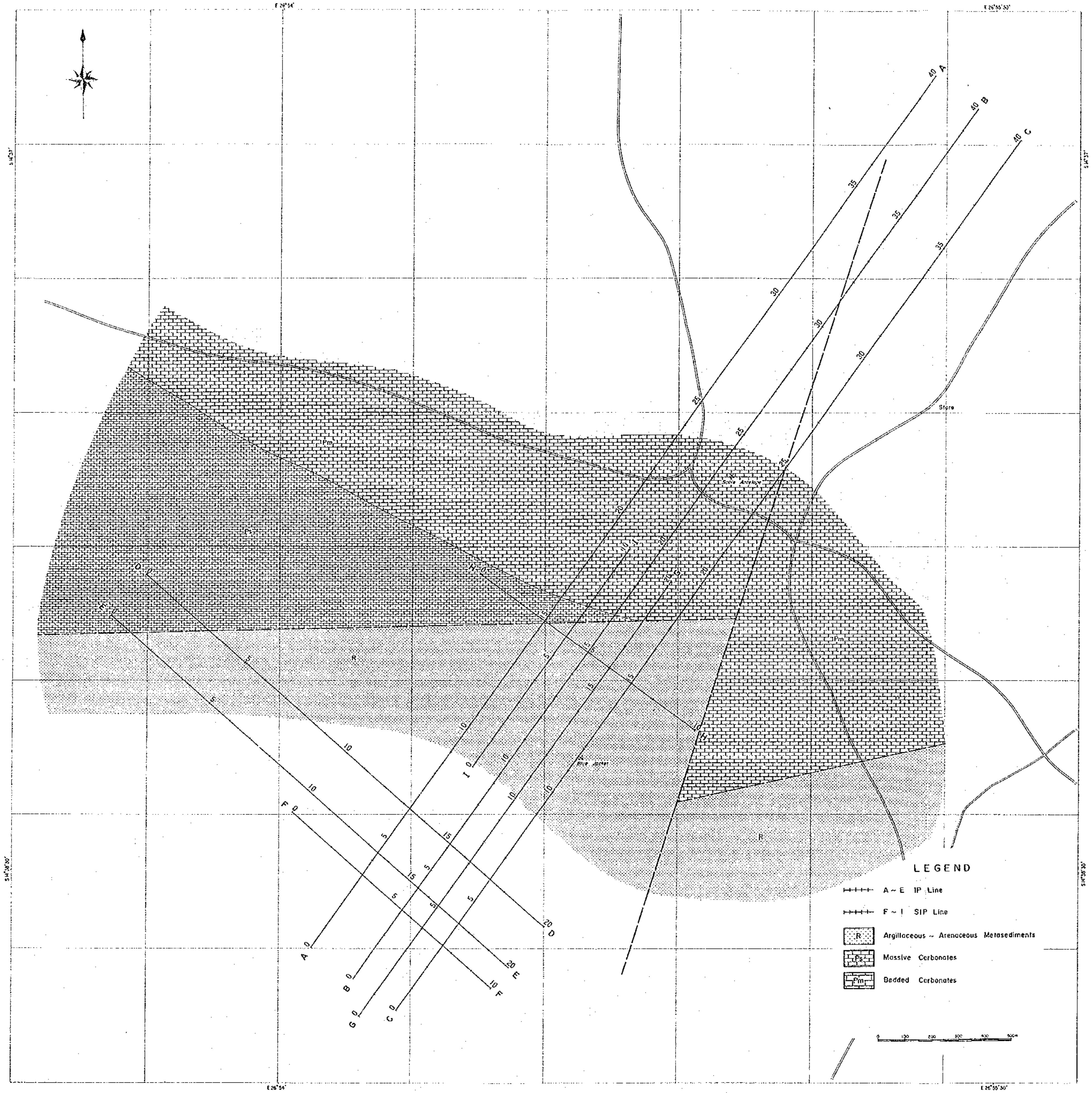

Fig. 14 Location Map IP and SIP Survey Lines

Line Lengths: Four lines totalling 5 km

Line F	1km
Line G	2km
Line H	1km
Line I	1km

1-4 Survey Method

In this survey of frequency-domain IP, the difference of apparent resistivities measured at two frequencies, viz., 0.125 and 1.0 Hz, is expressed in percentage. The field parameters such as electrode configuration, electrode separation and electrode separation index, etc. and field equipments are the same with those of SIP method.

In the SIP method, the magnitude and phase lag of IP response are measured at a broad range of frequencies from 0.01 to 100 Hz. The results are represented by a Cole-Cole diagram,a spectrum diagram of magnitudes and phases. Analysis of the frequency spectrum of IP response makes it possible to discriminate a type of mineralization or to eliminate electromagnetic coupling.

In this survey, the Harmonic System of Zonge (USA) was applied. Measurements are made using three standard waves of 0.125, 1.0 and 8.0 Hz, and the results are analysed using the Fast Fourier Transform (FFT). The IP responses over a range from 0.125 to 88 Hz are obtained through calculation of responses at frequencies of 3, 5, 7, 9 and 11 times higher than the standard waves.

In the SIP method, phase lag between transmitted current and received voltage is measured and thus, the transmitter and the receiver are synchronized through a communication wire.

1-5 Field Equipment

A set of field equipments for this survey is listed in Table 3. Block diagrams of the IP and the SIP sets are illustrated in Figs. 15 and 16 respectively.

2. Data Processing & Laboratory Investigation

2-1 IP method

The percent frequency effect and apparent resistivity were plotted on pseudosections of each line and compiled on plane figures of each electrode separation index number.

(1) Percent frequency effect

The percent frequency effect (PFE) is given by

$$PFE = \frac{M_{0.125Hz} - M_{1.0Hz}}{M_{1.0Hz}} \times 100\% \quad \text{---------(1)}$$

where $M_{0.125Hz}$, $M_{1.0Hz}$ are magnitudes measured at frequencies of 0.125 and 1.0Hz.

(2) Apparent resistivity

The apparent resistivity (AR) is given by

$$AR = \pi an(n+1)(n+2)\ V/I \quad \text{(ohm-m)} \quad \text{-------(2)}$$

where a: electrode separation in meter

n: electrode separation index

Table 3 IP・SIP Equipments (Zonge, Inc)

Equipment	Model	Specification	Qty
Power Supply	ZMG-5	Maximum Power: 5 kw Alternator: 400Hz,115V Engine: Honda G400 10Hp	1
Regulator	VR-1	Voltage Regulation	1
Transmitter	GGT-5	Output voltage: 250,500 750, 1000V Output current: Max 20A Square Wave Frequency : DC∿10KHz	1
Controller	XMT-12	Frequency : DC∿2,048Hz	1
Receiver	GDP-12/2GB	2 Channel Data Processor	1
Cassette/ Printer	CAP-12	Printer, Minicassette	1
Isolation Amp	ISO/1		2
Field Preamp	FP-1		2
Oscilloscope	Tektronix 212	2 channel	1
Electrode		Transmitter: Copper net, steel rod Receiver : Cu-$CuSO_4$ non polarizable pot	
Cable		Transmitter: VSF 1.25 mm^2	$12,000^m$
		Receiver: Shield Cable	$2,000^m$

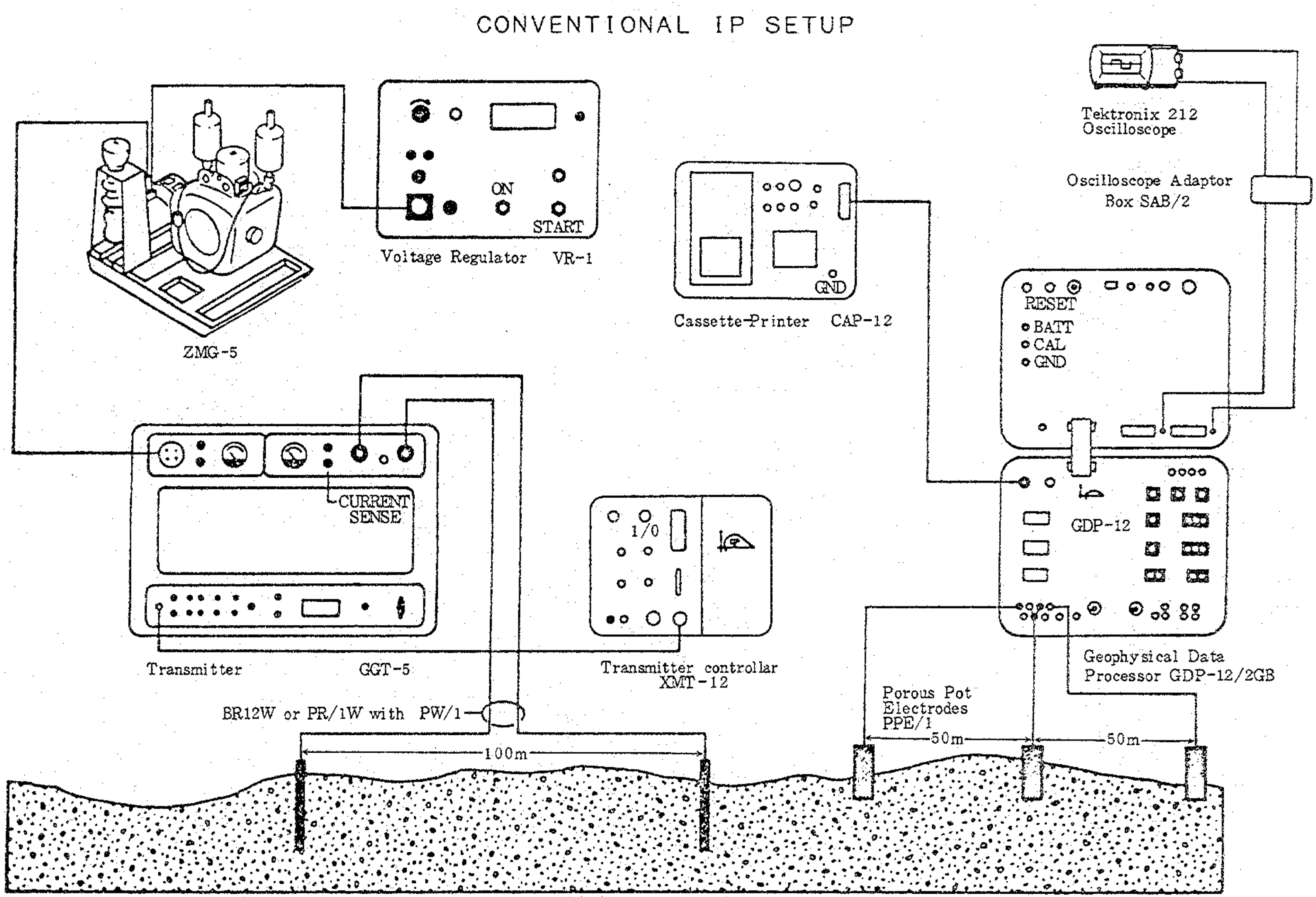

Fig. 15 Block Diagram of Zonge IP Survey System

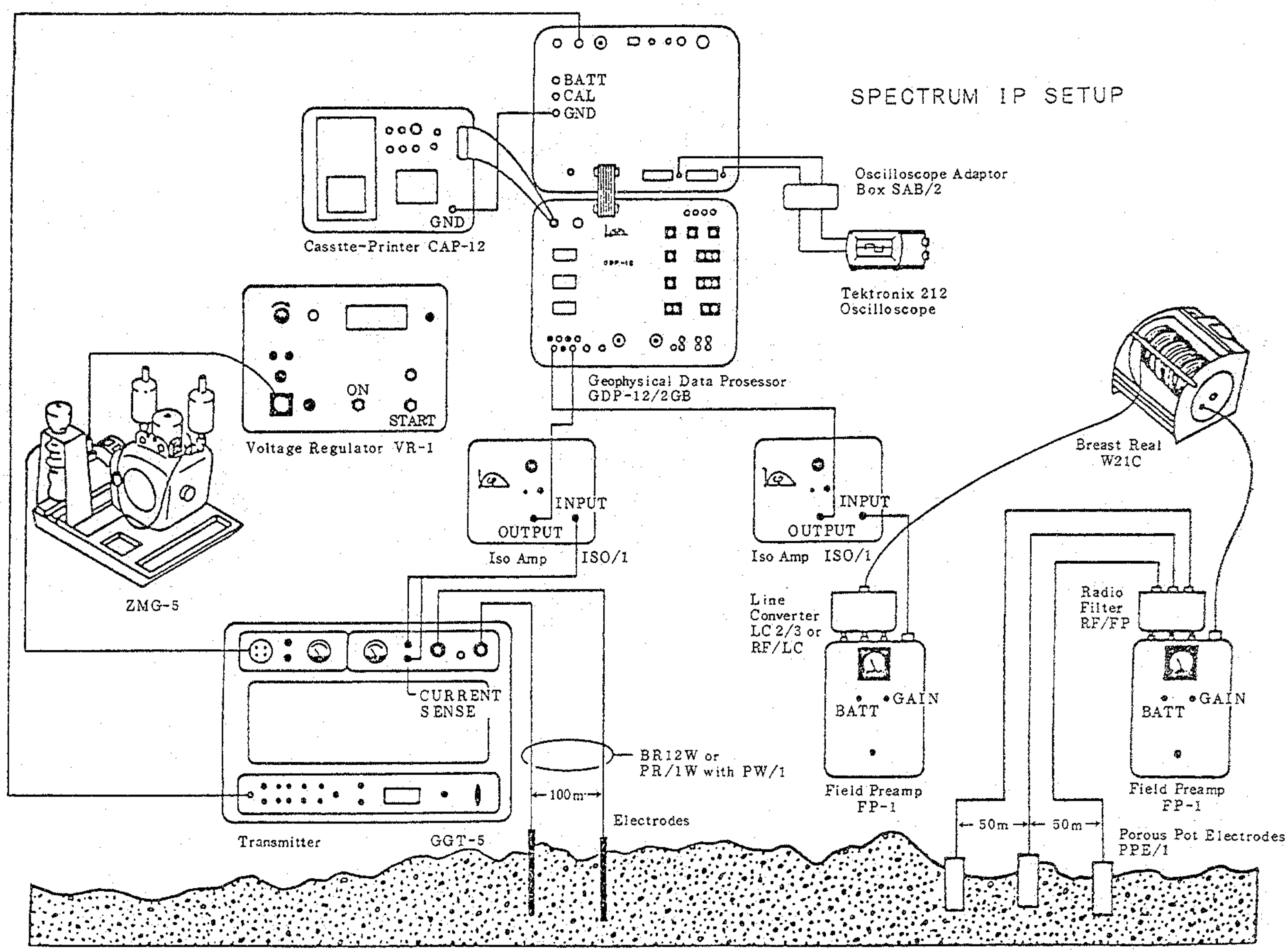

Fig. 16 Block Diagram of Zonge SIP Survey System

V: received voltage in volt

I: transmitted current in ampere

and in this survey,

a = 100m

n = 1 to 5

and V means the magnitude at the frequency of 0.125Hz.

2-2 SIP method

The output of the results comprises a series of real part and imaginary part of complex impedance of IP response which are measured over three standard waves of 0.125, 1.0 and 8.0Hz. Output are also the magnitude of the standard waves, the phase lag, the apparent resistivity and the frequency effect which is calculated with magnitudes of the standard wave, the seventh and the ninth harmonics. From these data,

(1) Cole-Cole Diagram

(2) Magnitude Spectrum

(3) Phase Spectrum

(4) Raw Phase

(5) PFE Pseudosection

(6) AR Pseudosection, etc.,

can be provided.

Some examples are given as follows.

(1) Cole-Cole Diagram

In a Cole-Cole diagram, printed-out data of each frequency are plotted in coordinates, of which the abscissa is the real number component and the ordinate is the imaginary number component. An example is shown in Fig.17. The Θi and Mi are called a phase and a magnitude respectively. The Cole-Cole diagram is known to display a spectral feature depending on some specific minerals or rocks.

(2) Magnitude Spectrum

The magnitude Mi or Mj in Cole-Cole diagram is normalized by being divided with the magnitude (Mo) of the minimum frequency 0.125Hz. An example is shown in Fig. 17.

(3) Phase Spectrum

An example of a frequency spectrum of phases (Θi and Θj in Cole-Cole diagram)is shown in Fig. 17.

2-3 Decoupling

Decoupling denotes the removal of electromagnetic coupling effects which are encountered in the SIP measurements. A decoupling procedure of this investigation is based on a method provided by P.G. Hallof and W. H. Pelton. The analytical method is summarized as follows.

A complex impedance $Z_A(f)$ obtained in the SIP measurements is approximated by the following equation.

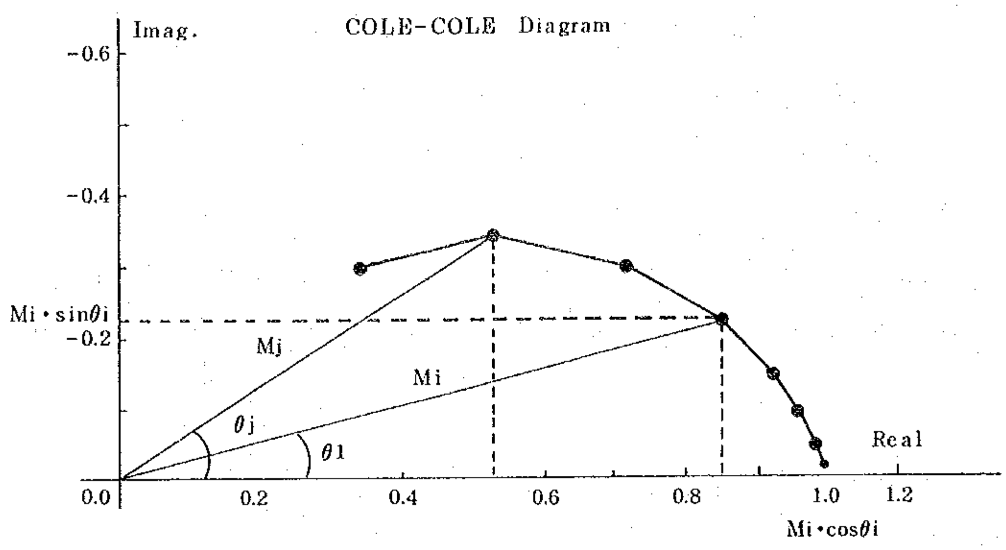

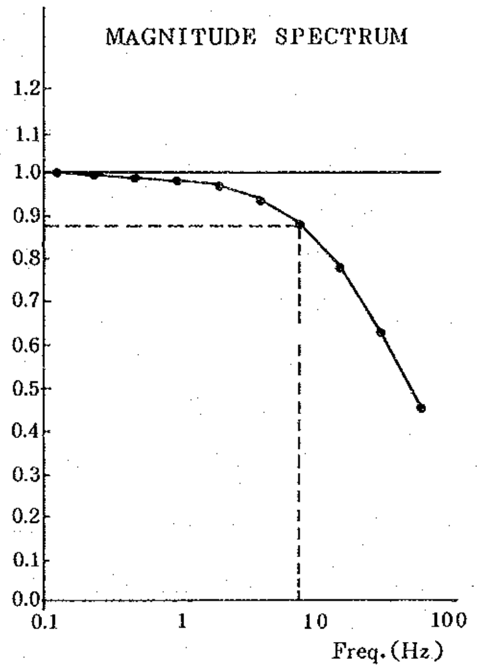

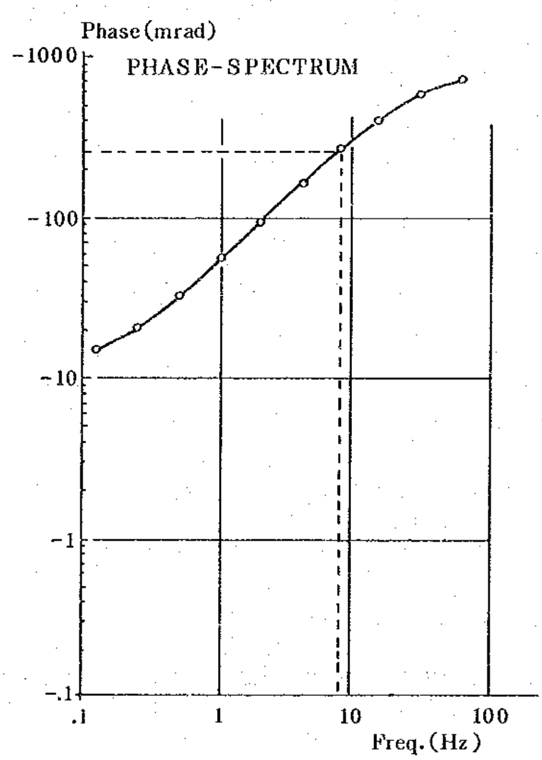

Fig. 17 Cole-Cole Diagram, Magnitude, Phase Spectrum

$$Z_A(f) = Ro[1 - m_1\{1 - \frac{1}{1 + (i2\pi f\tau)^{c_1}}\} - m_2\{1 - \frac{1}{1 + (i2\pi f\tau_2)^{c_1}}\}$$

$$+ m_3\{1 - \frac{1}{1 + (i2\pi f\tau_3)^{c_3}}\}] \quad ..(3)$$

where, m: chargeability

τ: time-constant

c: exponent of frequency

f: frequency.

The equation (3) comprises of three terms as follows.

$$1 - m_1\{1 - \frac{1}{1 + (i2\pi f\tau_1)^{c_1}}\} \quad ....(4)$$

$$-m_2\{1 - \frac{1}{1 + (i2\pi f\tau_2)^{c_2}}\} \quad ....(5)$$

$$+m_3\{1 - \frac{1}{1 + (i2\pi f\tau_3)^{c_3}}\} \quad ....(6)$$

The term(4) refers an IP response, the term(5) means electromagnetic coupling caused by a uniform earth and the term(6) represents a value of electromagnetic coupling caused by a conductor.

Ten parameters ($R_0, m_1, \tau_1, c_1, m_2, \tau_2, c_2, m_3, \tau_3, c_3$) of the equation (3) are determined from the SIP measurements using the non-linear least squares method. Being of the values of electromagnetic coupling, the terms (5) and (6) are removed from the equation (3) and the complex impedance $Z_{co}(f)$ is obtained from the IP response only.

$$Zco(f) = R_0[1-m_1\{1-\frac{1}{1+(i2\pi f\tau_1)^{c_1}}\}] \quad \ldots\ldots\ldots\ldots\ldots (7)$$

2-4 Laboratory Measurements

The SIP measurements have been conducted on the rocks and ores collected in the surveyed area. The results are summarized in Table 4. The Cole-Cole diagrams, the phase spectra and the magnitude spectra of the samples are shown in Fig. 18.

Ore samples have rather larger phase differences and PFE, and smaller apparent resistivities than those of rocks. The phase spectra of many ores comprising pyrite and chalcopyrite become smaller in accordance with increase of the frequency, whereas the phase spectrum of iron ore consisting of magnetite and hematite becomes larger with increase of the frequency. Distinct difference of phase spectrum will arise among ores depending on their constituents. On the contrary phase differences of rock samples are small and phase spectra of them give larger or rather constant phase differences when frequency is increased.

3. Results of Analyses

3-1 PFE and AR Pseudosections

Pseudosections of the percent frequency effect (PFE) and the apparent resistivity (AR) were provided over nine traverse lines from line A to line I.

Table 4 Electrical Property of Rock and Ore Samples

Sample No.	Rock, Ore	Resistivity 0.125 Hz (Ohm-m)	P F E 0.125-1 Hz (%)	Phase 0.125 Hz (-mrad)	Type of Spectrum	Location	Remarks
2	Bedded Limestone	30034	2.7	19.1	A	Line A 25	
7	Massive Dolonite	22555	0.4	2.5	A	Line B 16	
8	Colcareous Shale	1266	1.2	9.6	B	Line C 15	
9	Quartzite	13679	0.4	3.1	B	Line C 11.5	
10	Brecciated Dolomite	8363	0.3	1.6	A	Line C 7	
12	Massive Dolomite	14102	0.3	2.6	A	Line D 7	
6	Brecciated Dolomite	12142	0.2	2.4	A	Line C 20	
13	"	3914	1.3	9.6	B	Line B 23.5	
14	"	4127	1.9	12.6	B	Line B 23	
15	"	3812	1.1	2.3	B	Line B 24	
22	"	5093	4.2	25.6	B	Sable Antelope	Cp disseminated
23	"	6843	3.7	25.5	B	"	Cp,Py,Spc disseminated
25	"	8972	2.1	14.7	A	"	Py disseminated
16	Mineralized Brecciated Dolomite	718	82.6	421	Y	"	Cp,Py,Spc disseminated
17	"	104	94.8	477	X	"	"
18	"	99	200	715	X	"	"
19	"	6748	8.9	64.7	B	"	"
20	"	268	232	699	X	"	"
26	"	131	67.1	384	(X)	"	"
29	"	103	123	551	X	"	"
24	Mineralized Massive Dolomite	2465	2.1	15.4	B	"	Spc,Py disseminated
27	"	15454	5.3	37.8	B	"	Cp,Py,Bo disseminated
28	"	2978	6.3	43.0	Y	"	"
21	"	6966	4.6	32.1	C	"	Cp,Py,Spc disseminated
30	Ironoxide Ore	422	3.8	21.5	A	Line C 13.5	Mag, He

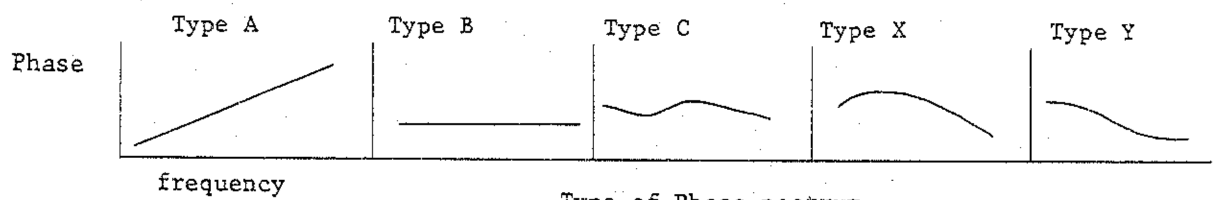

Type of Phase pectrum

NO. 2

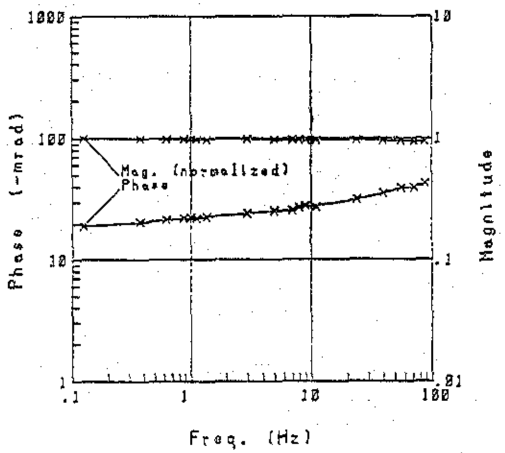

Spectrum type A
Bedded Limestone
Phase = 19.1 (-mrad)
PFE = 2.7 (%)
R = 30034 (ohm-m)

NO. 2 Cole-Cole Diagram

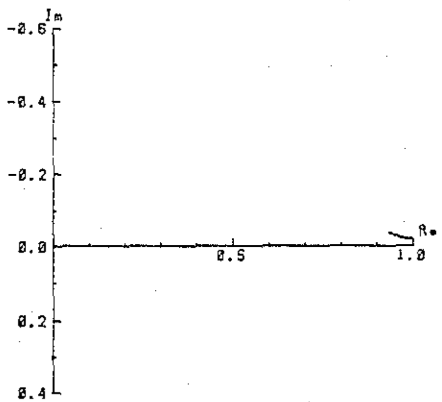

NO. 6

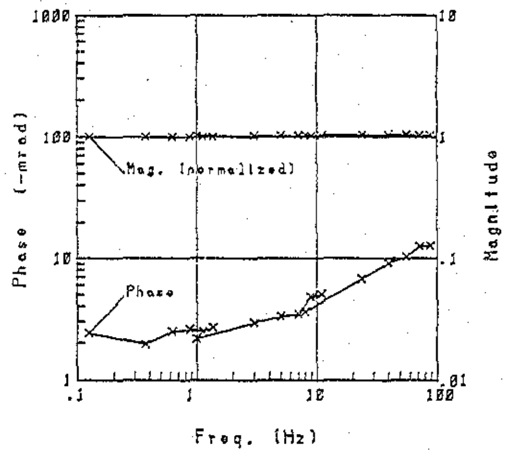

Spectrum type A
Brecciated Dolomite
Phase = 2.4 (-mrad)
PFE = 0.2 (%)
R = 12142 (ohm-m)

NO. 6 Cole-Cole Diagram

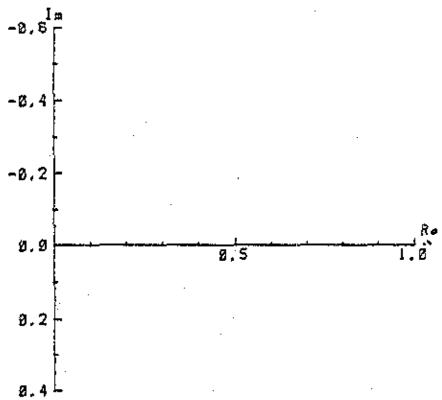

NO. 7

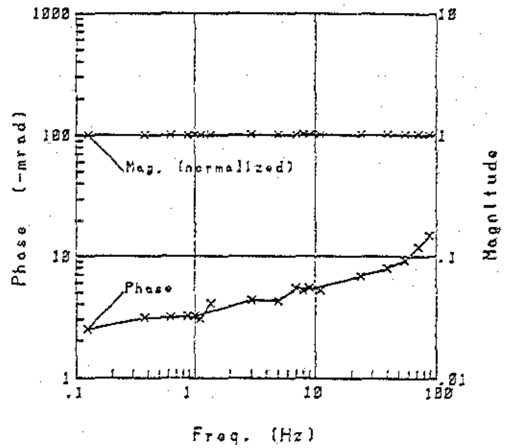

Spectrum type A
Massive Dolomite
Phase = 2.5 (-mrad)
PFE = 0.4 (%)
R = 22555 (ohm-m)

NO. 7 Cole-Cole Diagram

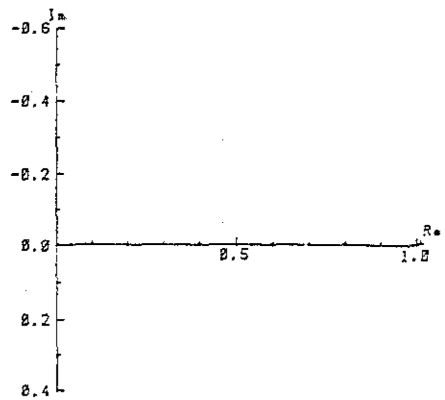

Fig. 18 Example of Phase, Magnitude, Cole-Cole Diagram of Ore

NO. 8

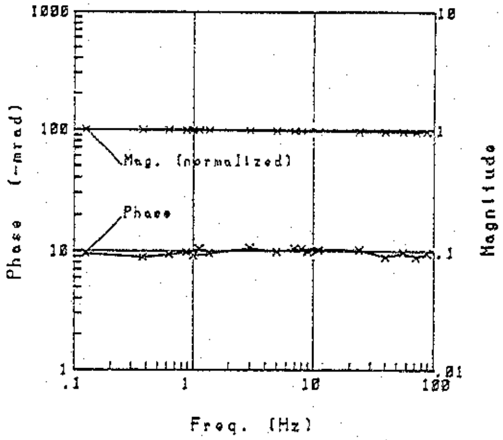

Spectrum type B
Calcareous Shale
Phase = 9.6 (-mrad)
PFE = 1.2 (%)
R = 1266 (ohm-m)

NO. 8 Cole-Cole Diagram

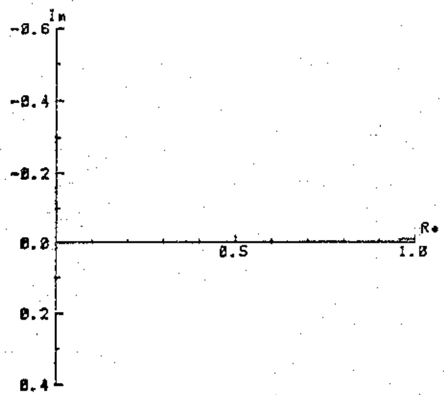

NO. 9

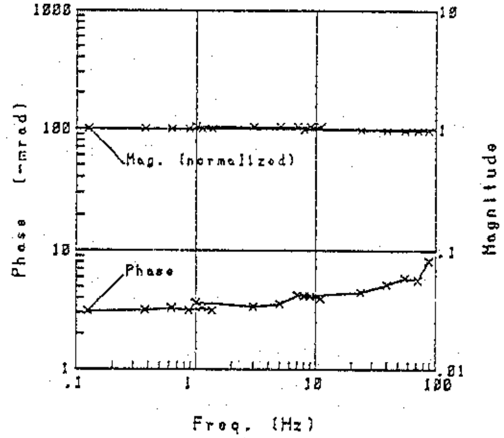

Spectrum type B
Quartzite
Phase = 3.1 (-mrad)
PFE = 0.4 (%)
R = 13679 (ohm-m)

NO. 9 Cole-Cole Diagram

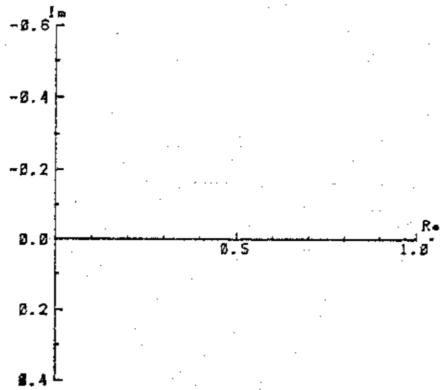

NO. 10

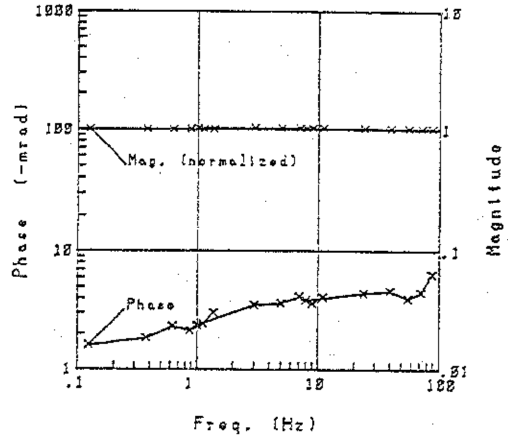

Spectrum type A
Brecciated Dolomite
Phase = 1.6 (-mrad)
PFE = 0.3 (%)
R = 8363 (ohm-m)

NO. 10 Cole-Cole Diagram

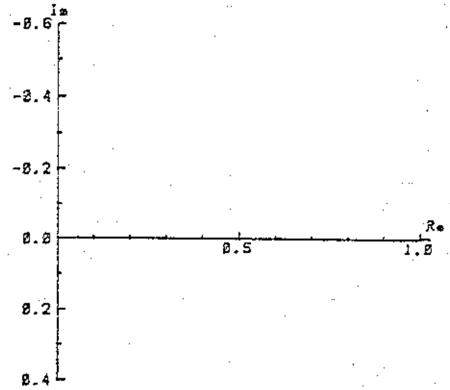

NO. 12

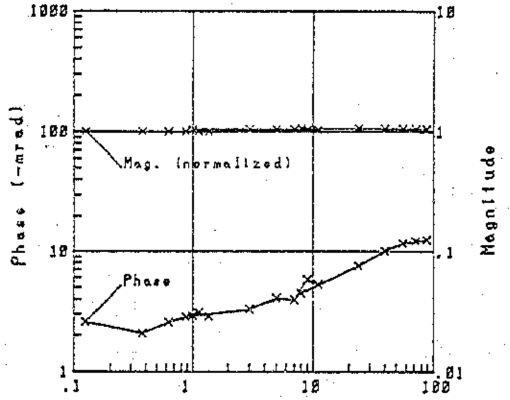

Spectrum type A
Massive Dolomite
Phase = 2.6 (-mrad)
PFE = 0.3 (%)
R = 14102 (ohm-m)

NO. 12 Cole-Cole Diagram

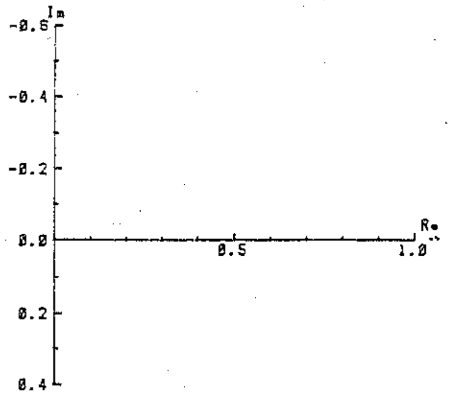

NO. 13

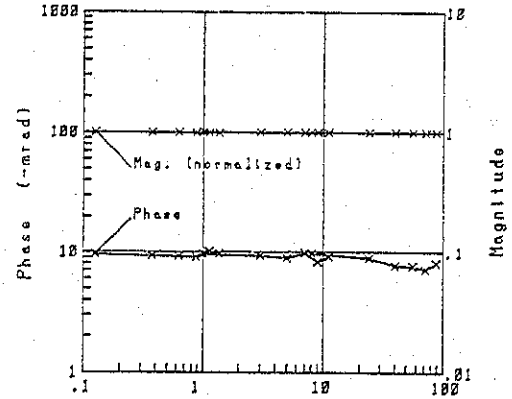

Spectrum type B
Brecciated Dolomite
Phase = 9.6 (-mrad)
PFE = 1.3 (%)
R = 3914 (ohm-m)

NO. 13 Cole-Cole Diagram

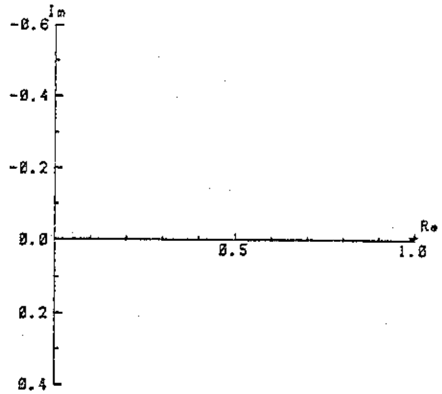

NO. 14

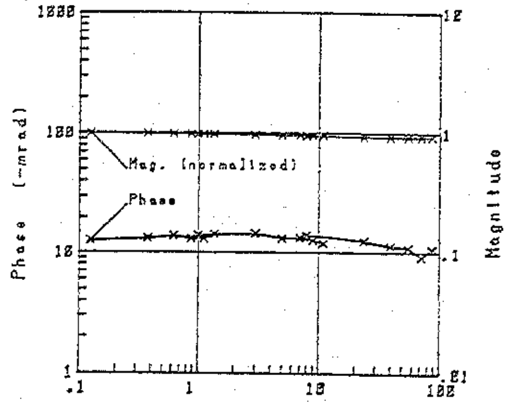

Spectrum type B
Brecciated Dolomite
Phase = 12.6 (-mrad)
PFE = 1.9 (%)
R = 4127 (ohm-m)

NO. 14 Cole-Cole Diagram

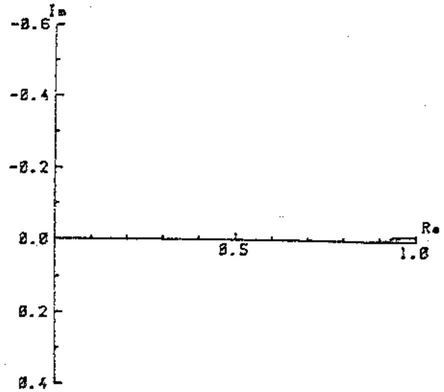

NO. 15

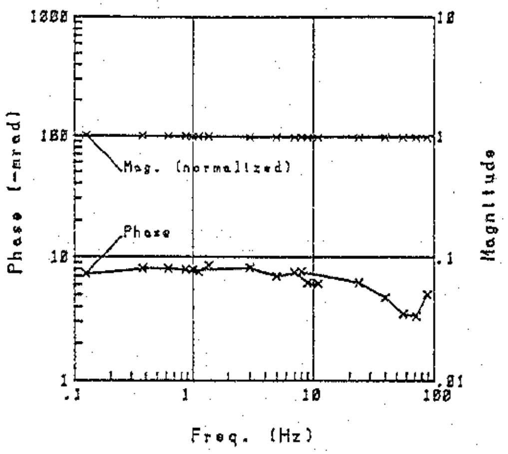

Spectrum type B
Brecciated Dolomite
Phase = 7.3 (-mrad)
PFE = 1.1 (%)
R = 3812 (ohm-m)

NO. 16

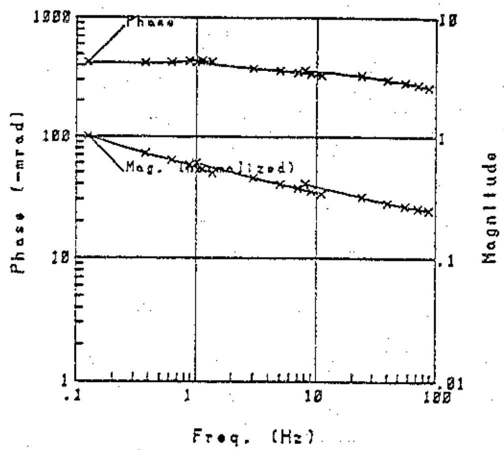

Spectrum type Y
Mineralized Brecciated Dolomite
Phase = 421 (-mrad)
PFE = 82.6 (%)
R = 718 (ohm-m)

NO. 17

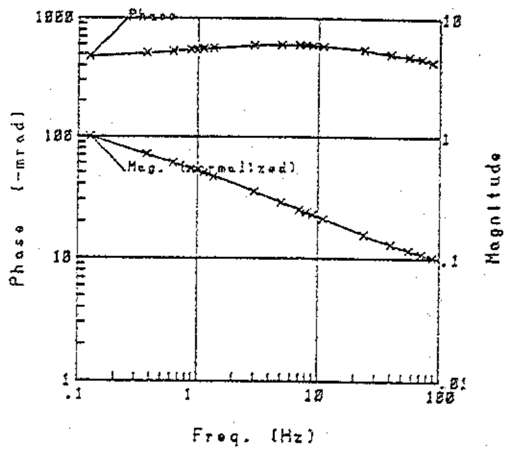

Spectrum type X
Mineralized Brecciated Dolomite
Phase = 477 (-mrad)
PFE = 94.8 (%)
R = 104 (ohm-m)

NO. 15 Cole-Cole Diagram

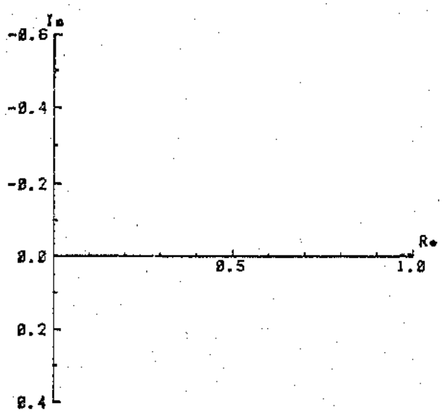

NO. 16 Cole-Cole Diagram

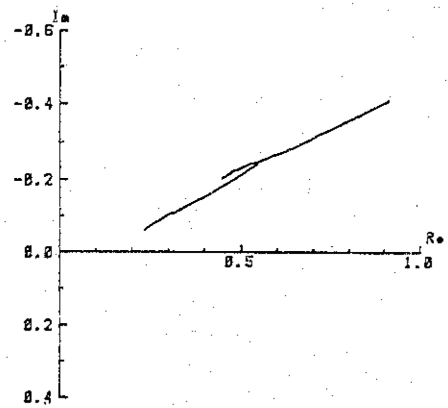

NO. 17 Cole-Cole Diagram

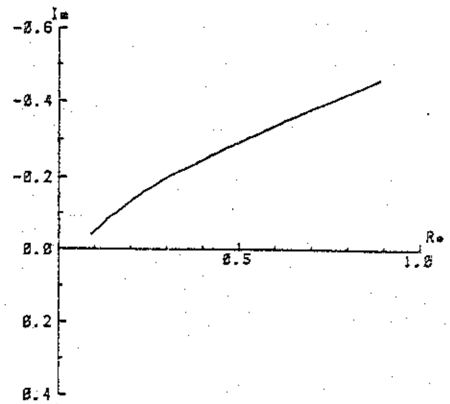

NO. 18

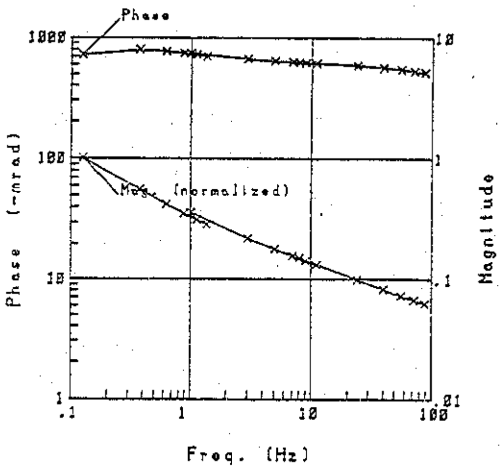

Spectrum type X
Mineralized Brecciated Dolomite
Phase = 715 (-mrad)
PFE = 200 (%)
R = 99 (ohm-m)

NO. 18 Cole-Cole Diagram

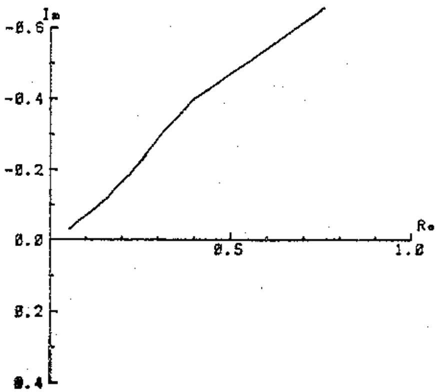

NO. 19

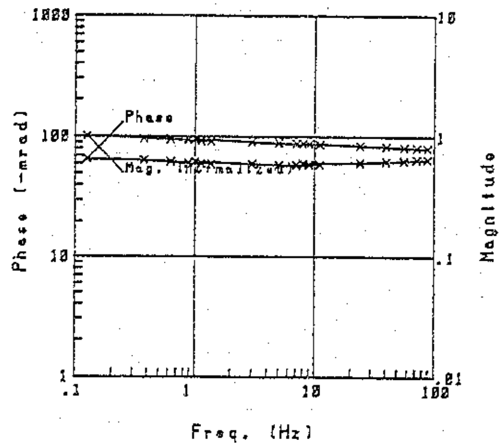

Spectrum type B
Mineralized Brecciated Dolomite
Phase = 64.7 (-mrad)
PFE = 8.9 (%)
R = 6748 (ohm-m)

NO. 19 Cole-Cole Diagram

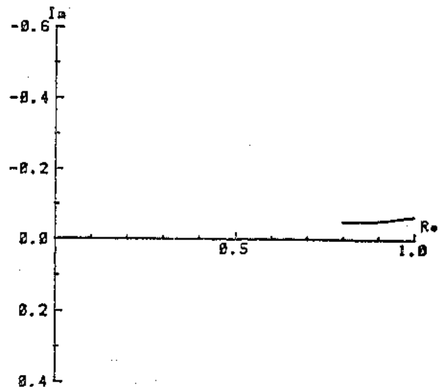

NO. 20

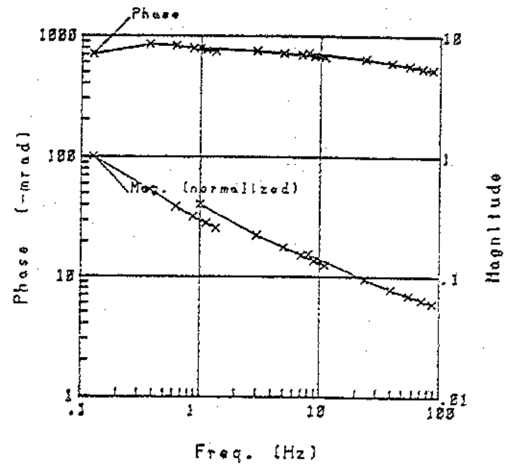

Spectrum type X
Mineralized Brecciated Dolomite
Phase = 699 (-mrad)
PFE = 232 (%)
R = 268 (ohm-m)

NO. 20 Cole-Cole Diagram

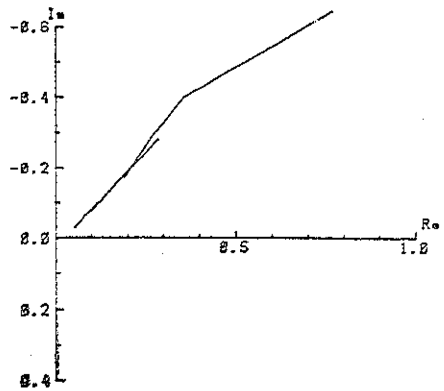

NO. 21

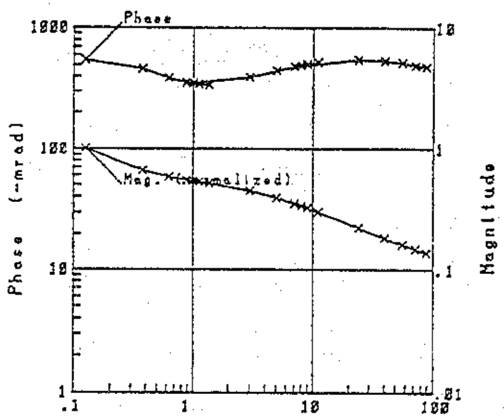

Spectrum type C
Mineralized Massive Dolomite
Phase = 32.1 (-mrad)
PFE = 4.6 (%)
R = 6966 (ohm-m)

NO. 21 Cole-Cole Diagram

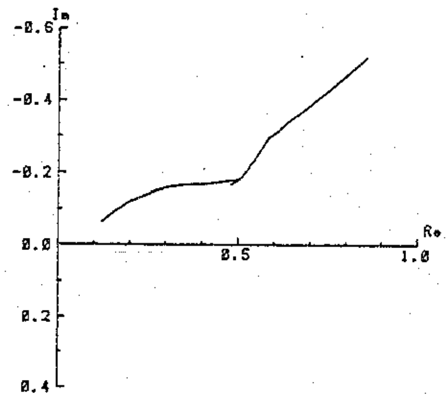

NO. 22

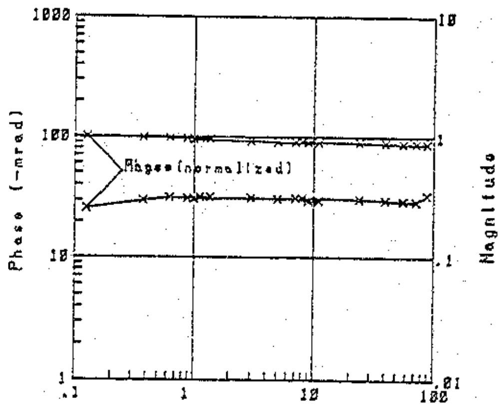

Spectrum type B
Brecciated Dolomite
Phase = 25.6 (-mrad)
PFE = 4.2 (%)
R = 5093 (ohm-m)

NO. 22 Cole-Cole Diagram

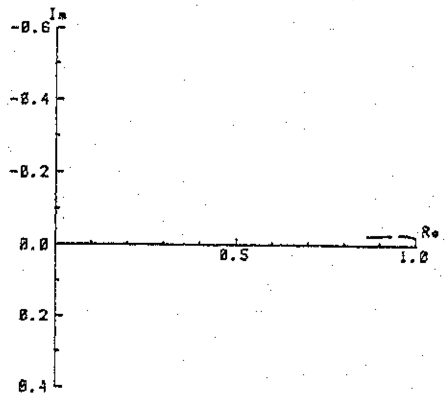

NO. 23

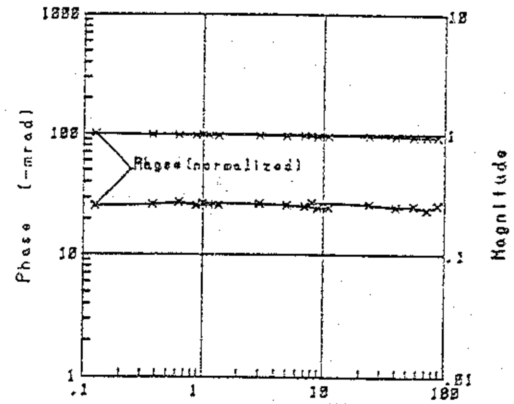

Spectrum type B
Brecciated Dolomite
Phase = 25.5 (-mrad)
PFE = 3.7 (%)
R = 6843 (ohm-m)

NO. 23 Cole-Cole Diagram

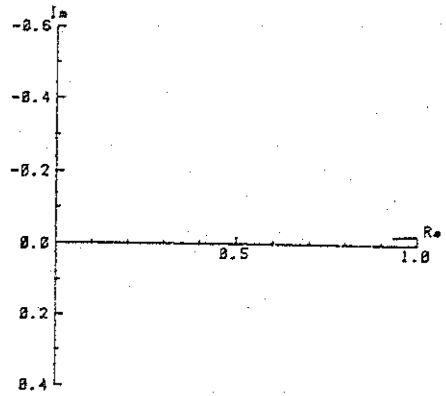

NO. 24

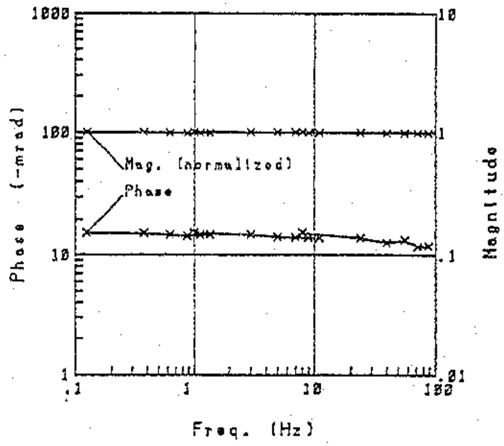

Spectrum type B
Mineralized Massive Dolomite
Phase = 15.4 (−mrad)
PFE = 2.1 (%)
R = 2465 (ohm−m)

NO. 24 Cole-Cole Diagram

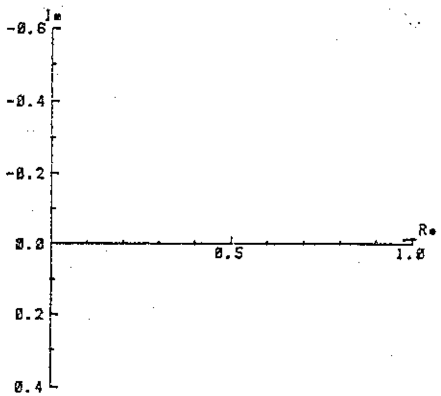

NO. 25

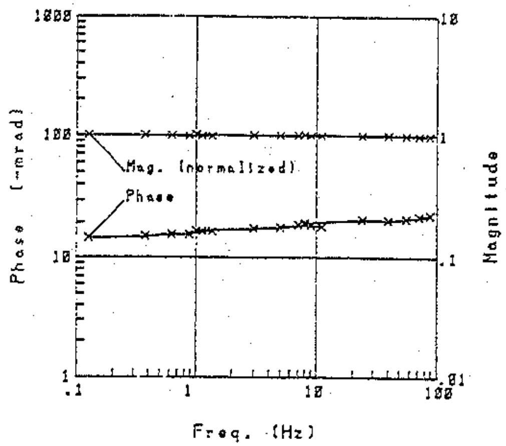

Spectrum type A
Brecciated Dolomite
Phase = 14.7 (−mrad)
PFE = 2.1 (%)
R = 8972 (ohm−m)

NO. 25 Cole-Cole Diagram

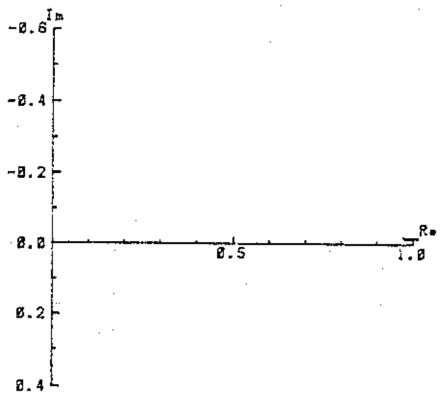

NO. 26

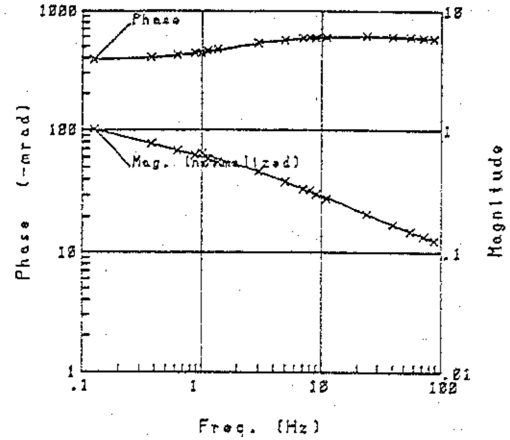

Spectrum type X
Mineralized Brecciated Dolomite
Phase = 384 (−mrad)
PFE = 67.1 (%)
R = 131 (ohm−m)

NO. 26 Cole-Cole Diagram

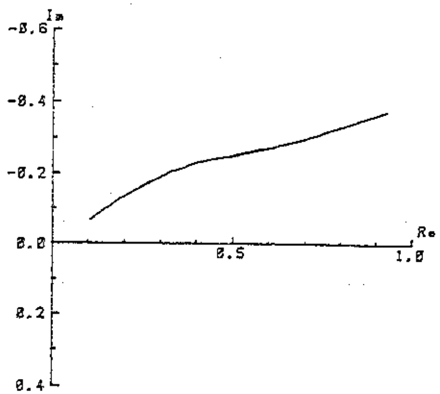

NO. 27

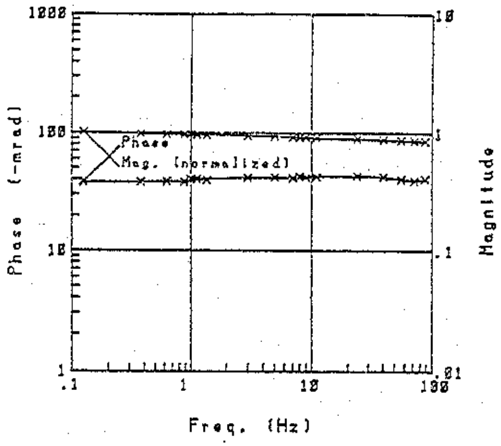

Spectrum type B
Mineralized Massive Dolomite
Phase = 37.8 (−mrad)
PFE = 5.3 (%)
R = 15454 (ohm−m)

NO. 27 Cole-Cole Diagram

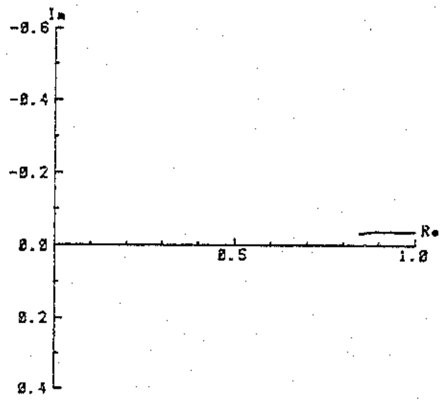

NO. 28

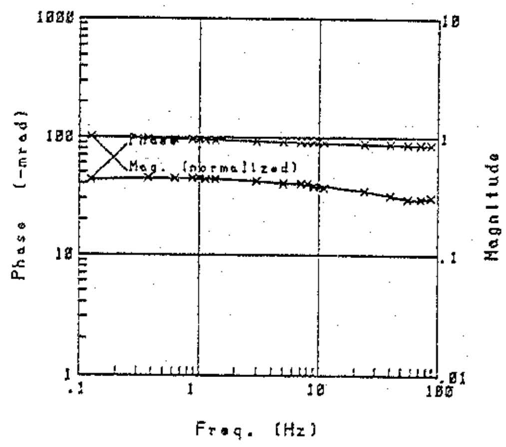

Spectrum type Y
Mineralized Massive Dolomite
Phase = 43.0 (−mrad)
PFE = 6.3 (%)
R = 2978 (ohm−m)

NO. 28 Cole-Cole Diagram

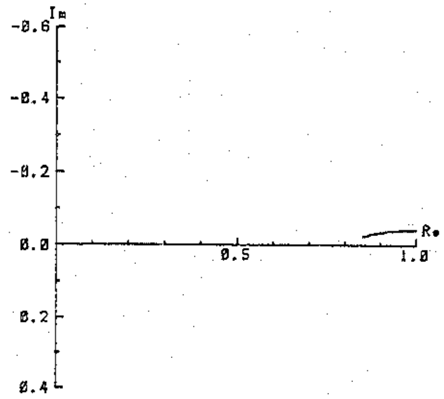

NO. 29

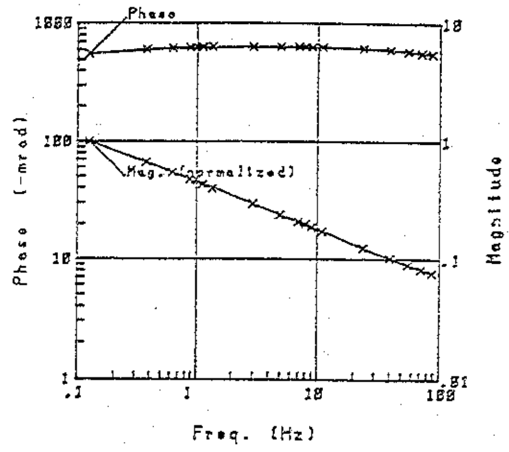

Spectrum type X
Mineralized Brecciated Dolomite
Phase = 551 (−mrad)
PFE = 123 (%)
R = 103 (ohm−m)

NO. 29 Cole-Cole Diagram

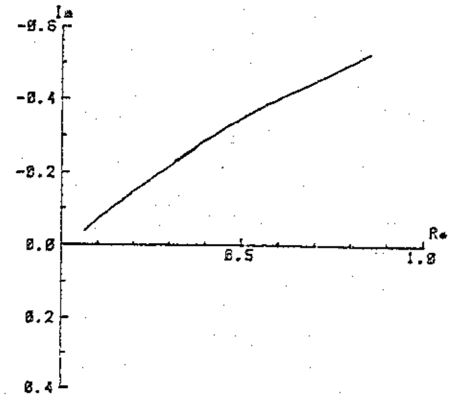

NO. 30

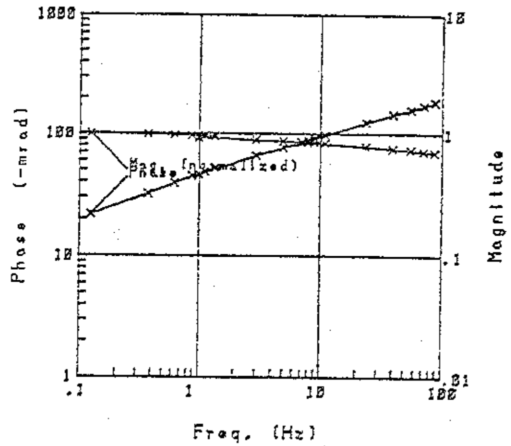

Spectrum type A
Iron oxide ore
Phase = 21.5 (−mrad)
PFE = 3.8 (%)
R = 422 (ohm−m)

NO. 30 Cole-Cole Diagram

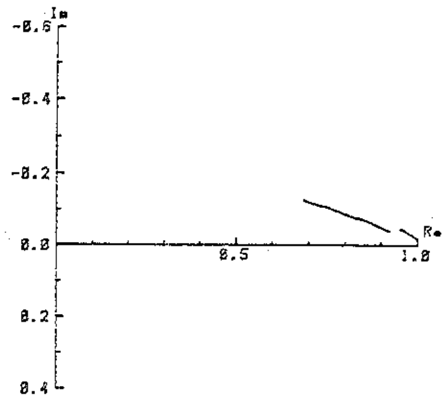

(1) Line A (Fig. 19)

Anomalies of PFE were detected at three sections, between stations 2 and 5, between stations 14 and 15, and at station 23.

The strong anomaly of more than 5% PFE between stations 2 and 5 is situated in the area of metasediments. The apparent resistivity ranges from 10 to 100 ohm-m and it appears to become less resistive to the southwestern end of the line.

The anomaly between stations 14 and 15 lies in the vicinity of a boundary of limestones with metasediments and has a strong PFE of more than 5%. The apparent resistivity of the anomaly ranges from 300 to 600 ohm-m in the background values of more than 1,000 ohm-m and gives a good contrast of resistivities.

The anomaly at station 23 exists on limestones and has a weak PFE of the order of 2%. The apparent resistivity is remarkably high being more than 10,000 ohm-m and the anomaly can be deemed to rest within highly resistive rocks.

(2) Line B (Fig. 19)

Four anomalies of PFE have been detected between stations 2 and 5, at stations 15, 24 and 28.

The anomaly between stations 2 and 5 is in metasediments and has a strong PFE of more than 5%. The apparent resistivity ranges from 10 to 100 ohm-m and has a tendency to diminish towards the southwestern end of the traverse line.

The anomaly at station 15 is situated on the boundary between limestones and metasediments and of more than 5%PFE. The apparent resistivity of this anomaly ranges from 300 to 600 ohm-m in the background values of more than 1,000 ohm-m. The PFE, AR and its pattern of this anomaly are similar to those of the section between stations 15 and 16 on line A.

(3) Line C (Fig. 20)

Anomalous PFE were observed between stations 2 and 7, and at stations 15, 24 and 28.

The anomaly between stations 2 and 7 lies on metasediments and has a strong PFE of more than 5%. The apparent resistivity is less than 100 ohm-m. At the southwestern end of the line, the apparent resistivity is extremely low being less than 10 ohm-m. This anomalous section seems to be continuous with the anomalies observed between stations 2 and 5 on both lines A and B.

The anomaly at station 15 stands at more than 5%PFE on a boundary between limestones and metasediments. The apparent resistivity of the anomalous section ranges from 300 to 600 ohm-m in contrast with the background values of not less than 1,000 ohm-m. The value and pattern of this anomaly resembles to those of at station-15's on both lines A and B, suggesting that these anomalies were originated from the same anomalous zone.

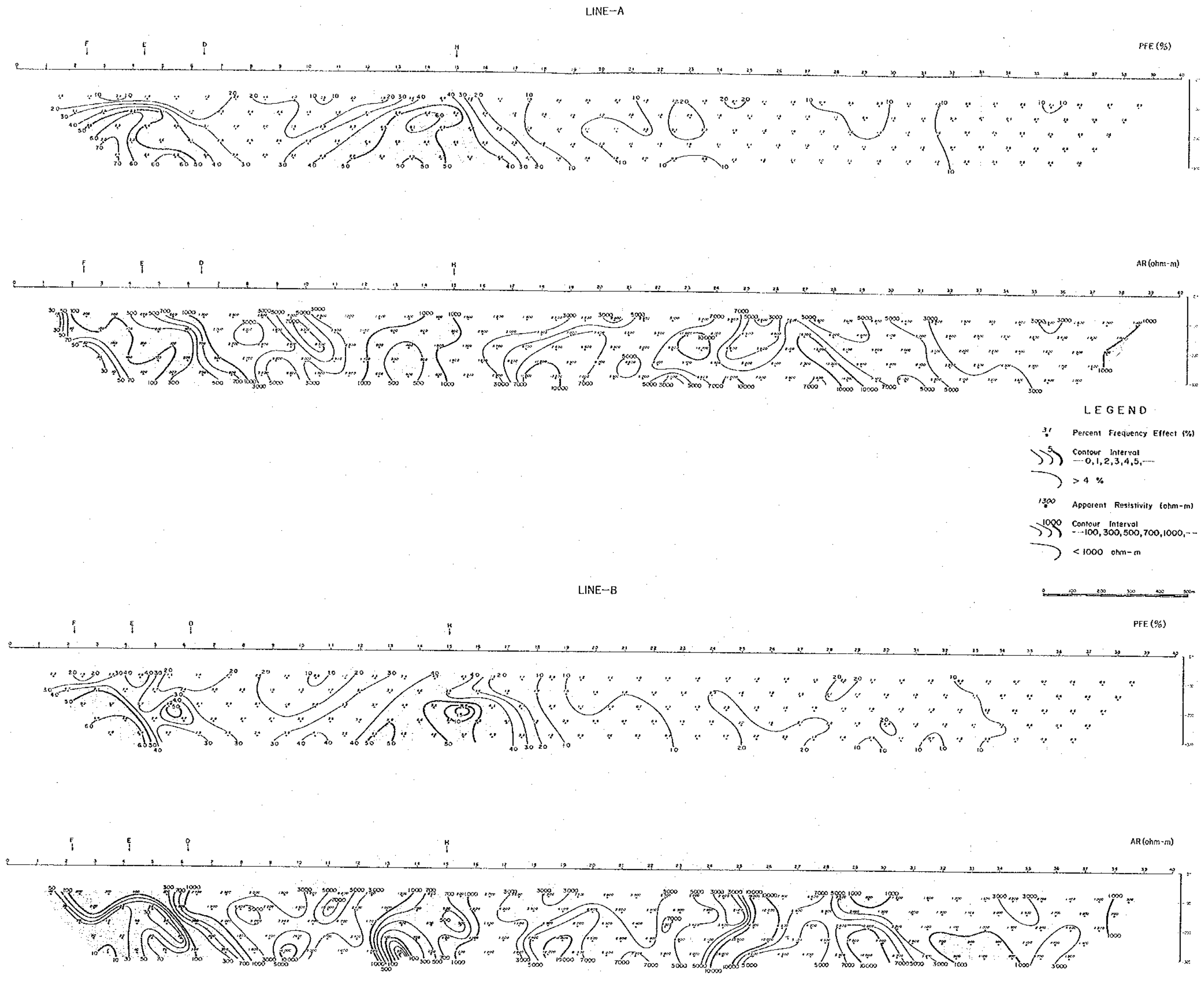

Fig. 19 Pseudo-Section Lines A, B

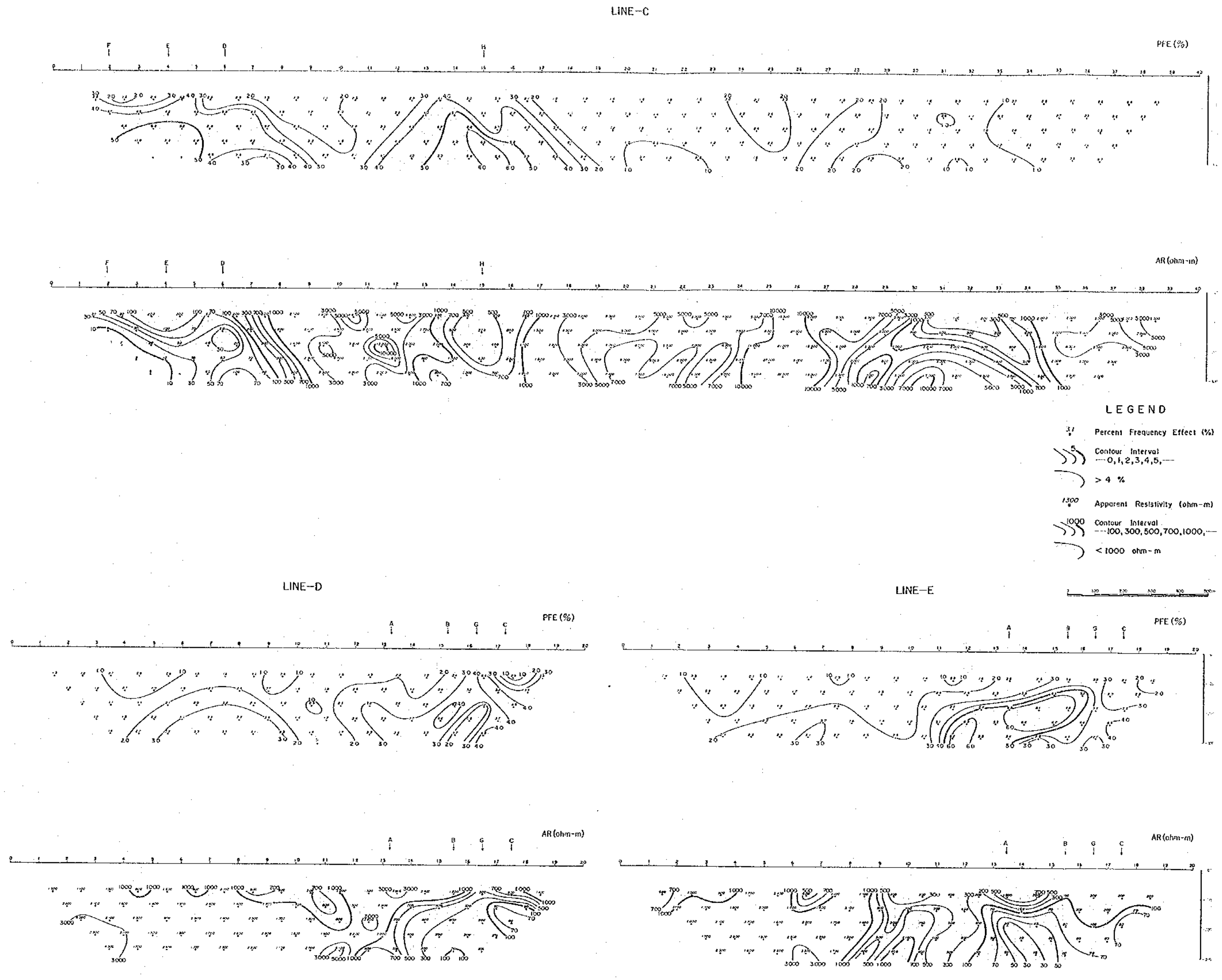

Fig. 20 Pseudo-Section Lines C, D, E

The anomalies at stations 24 and 28 lie on limestones and are of the order of 2%PFE. They are anomalies in highly resistive rocks with the values of 5,000 to 9,000 ohm-m. Among anomalies within highly resistive rocks, those of at stations 23 on line A, 24 on line B and 24 on line C may be continuative. Also, the anomalies at station 28s on both lines B and C are perceptible to have been linked in a line.

(4) Line D (Fig. 20)

Anomalies of PFE were delineated between stations 7 and 8 and stations 16 and 17.

The anomaly between stations 7 and 8 is in the area of metasediments and in the order of 3%PFE with the high apparent resistivities from 1,000 to 2,000 ohm-m. The depth of anomalous zone is deemed to exceed 200m.

The anomaly between stations 16 and 17 is found in metasediments and has a moderately intensive PFE of some 4% with the apparent resistivity of 200 to 300 ohm-m. This anomaly forms a part of anomalous zone detected between stations 2 and 5 of lines A, B and C.

(5) Line E (Fig. 20)

An anomaly of PFE is found between stations 12 and 16. This anomaly shows a strong PFE beyond 5% with the apparent resistivity less than 100 ohm-m and is correlative with the anomalies between stations 2 and 5 on lines A,B and C, and stations 16 and 17 on line D.

(6) Line F (Fig. 21)

The traverse lines F to I are for SIP measurements. A strong anomaly of some 5%PFE was detected within the area of metasediments between stations 3 and 8. The value of PFE is likely to increase with depths. The apparent resistivity is less than 100 ohm-m. Similarly to the anomaly between stations 16 and 17 on line D, this anomaly is a part of anomalous zone delineated in the vicinities of stations 2 to 5 of lines A,B and C.

(7) Line G (Fig. 21)

Two anomalies of PFE were delineated.

The anomaly between stations 2 and 7 in metasediments has a broad area of more than 5%PFE with the apparent resistivity of less than 100 ohm-m. At the southwestern end of the line, the area forms a zone of low resistivity not exceeding 10 ohm-m. This anomaly is a part of the anomalous zone at stations 3 to 8 on line F and at stations 2 to 5 on lines A,B and C.

The anomaly at station 15 on line G shows a strong PFE of the order of 5% in the vicinity of a boundary between limestones and metasediments. The apparent resistivity of the anomaly ranges from 300 to 700 ohm-m against a background value of more than 1,000 ohm-m. This anomaly is similar to

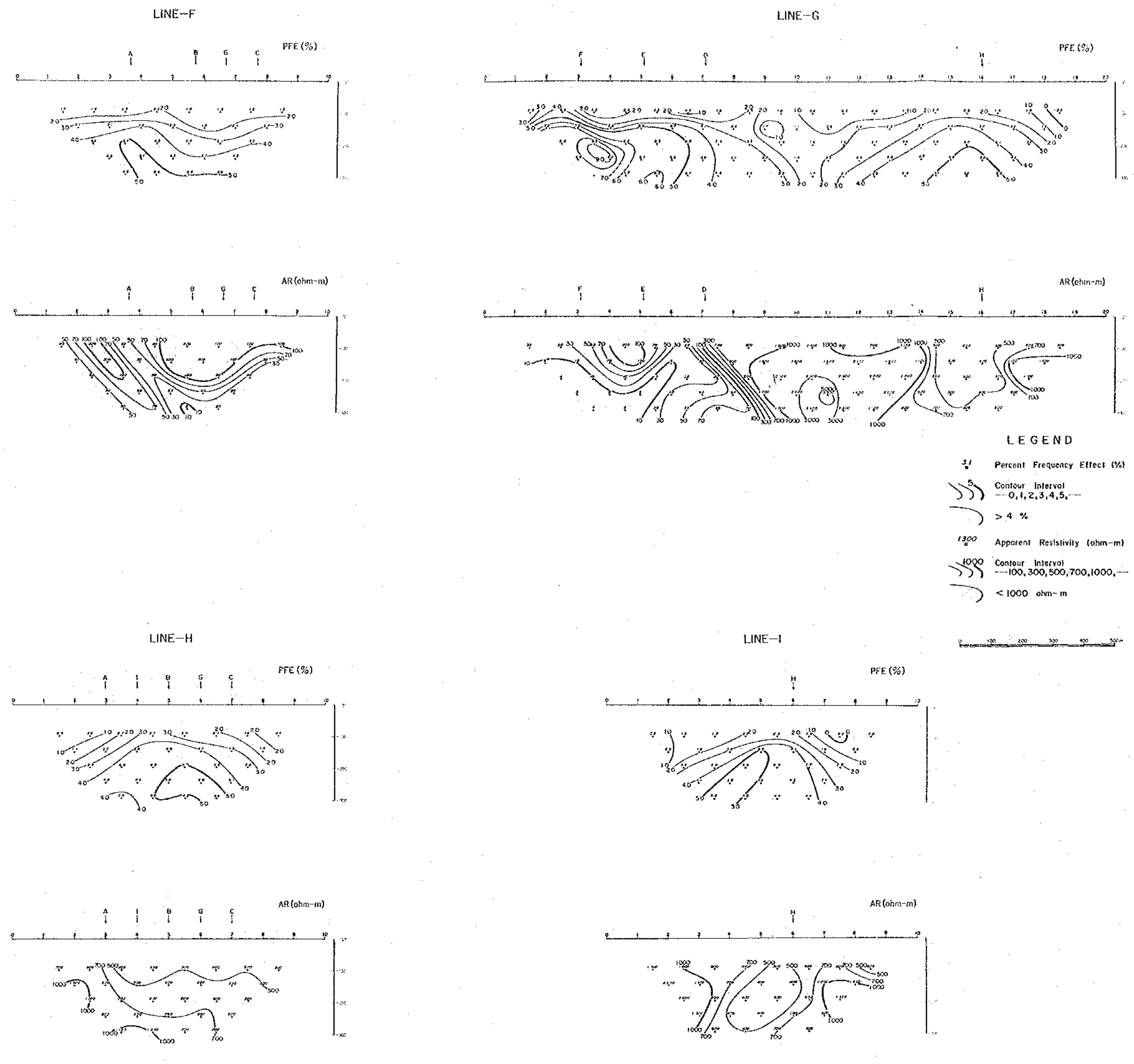

Fig. 21 Pseudo-Section Lines F, G, H, I

the anomaly at station 15s on lines A, B and C being originated in the same anomalous zone.

(8) Line H (Fig. 21)

The line H intersects lines A, B and C at each station 15 and line G at station 16.

A strong anomaly of some 5%PFE was detected between stations 4 and 6 on a boundary of limestones with metasediments. The anomalous values are similar to those observed on lines A,B,C and G. Apparent resistivity usually falls within a range of 500 to 700 ohm-m, indicating that this traverse line is on a zone of low resistivity.

(9) Line I (Fig. 21)

A strong anomaly of the order of 5%PFE was observed between stations 5 and 6 on a boundary of limestones with metasediments. The apparent resistivity ranges from 400 to 700 ohm-m against the background values of more than 1,000 ohm-m. This anomaly gave the values and a pattern similar to those observed in the vicinity of station 15s on lines A,B,C and G.

3-2 Contours of PFE and AR

The contours of RFE with a separation index n = 1,2,3,4 or 5 (Fig. 22 ∿ Fig. 26) and the contours of AR with a separation index n = 1,2,3,4 or 5 (Fig. 27 ∿ Fig. 31) were prepared.

The anomalies extracted from pseudosections of PFE and AR in the foregoing paragraph are shown as five zones of anomalies from No.1 to No.5 in plane figures. An explanation of these zones of anomalies is given on the plane figures of n=2 and 4.

(1) Contours of PFE, n=2 (Fig. 23)

The zones of anomalies from No.1 to No.4 are best illustrated in this figure. The zone No.1 is shown by a contour line of 2% which encloses station 28 on line B and station 28 on line C. The zone No.2 is shown by a contour line of 2% which surrounds stations 23 on line A, 24 on line B, and 24 and 25 on line C. These zones are located in limestones and the depths of the tops of anomalies are around 100m. They extend in WNW-ESE direction, particularly the zone No. 2 passing across the area of Sable Antelope.

The anomaly zone No.3 is defined by a contour line of 4% which covers an area of stations 13 to 15 on line A, 5 to 6 on line I, 14 to 15 on line B, 15 to 16 on line G, 13 to 14 on line C and 4 to 6 on line H. The zone No. 3 is situated within or on the boundary of metasediments surrounded by limestones. The apparent resistivity ranges from 300 to 600 ohm-m against the background values of more than 1,000 ohm-m. The anomaly zone extends in a WNW-ESE direction and a depth of top is estimated to be about 100m. The CSAMT method in the previous year detected this zone as a zone of low resistivity faulted on both east and west sides.

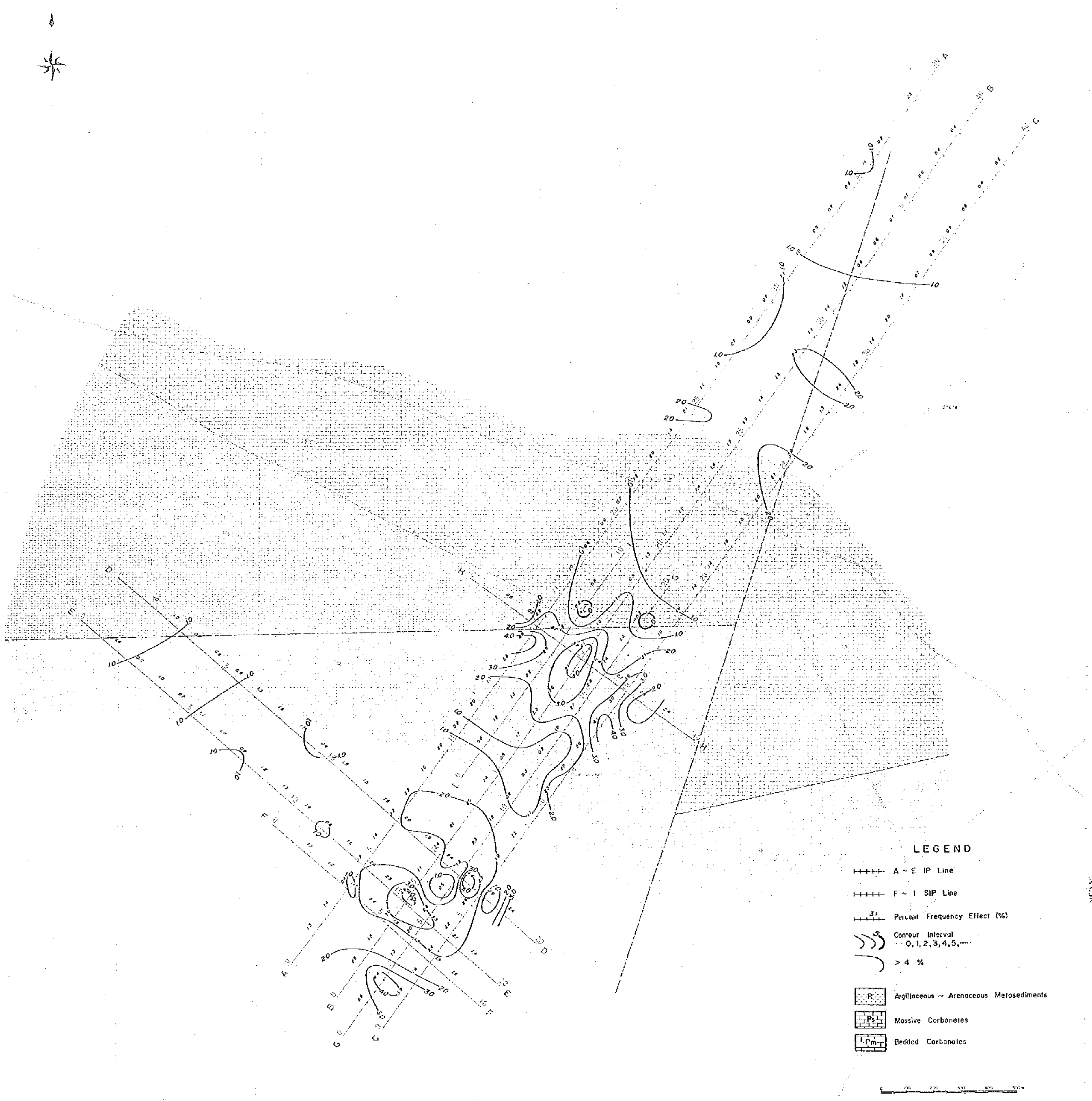

Fig. 22 Plan Map of Percent Frequency Effect [N=1]

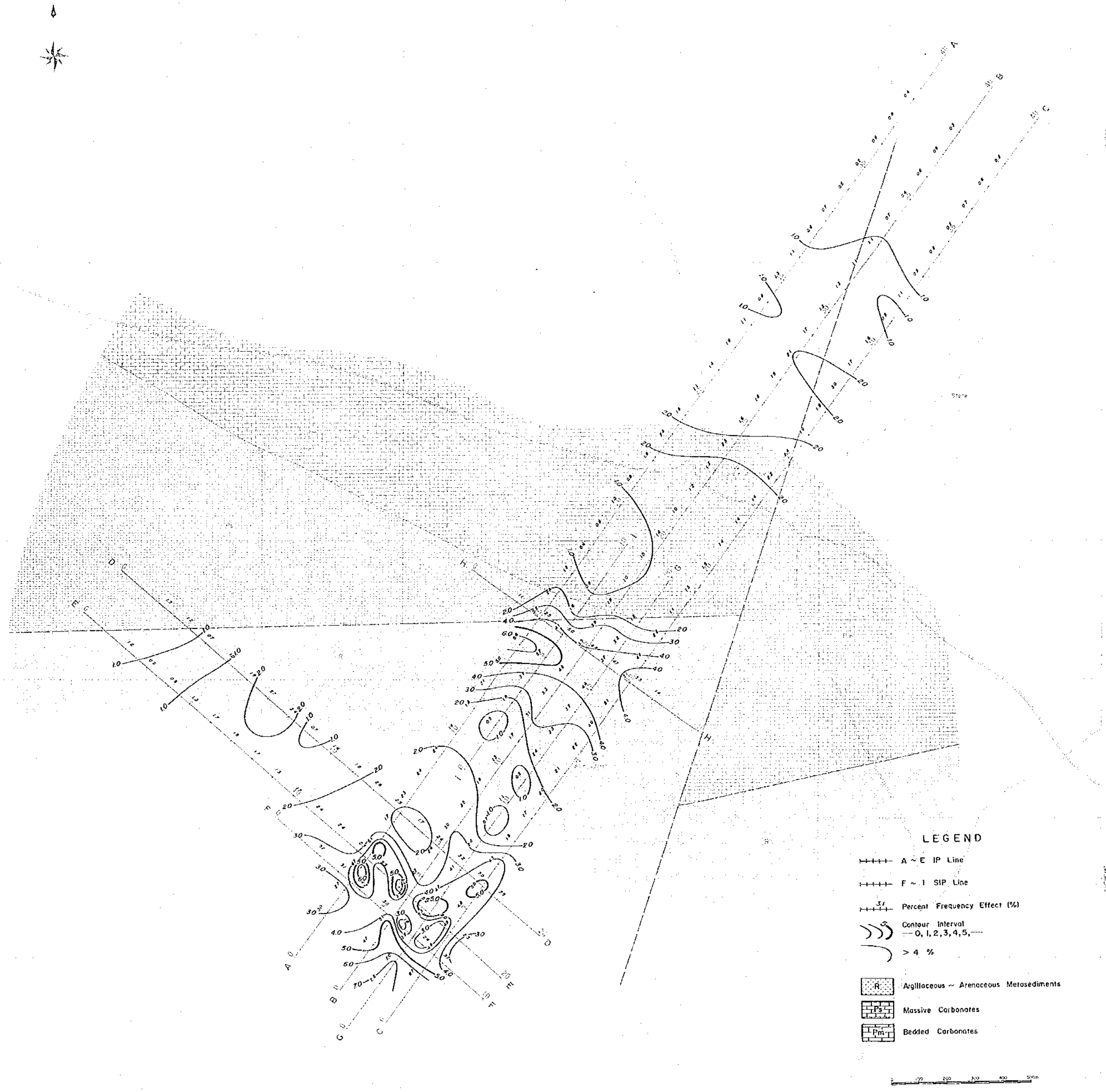

Fig. 23 Plan Map of Percent Frequency Effect [N=2]

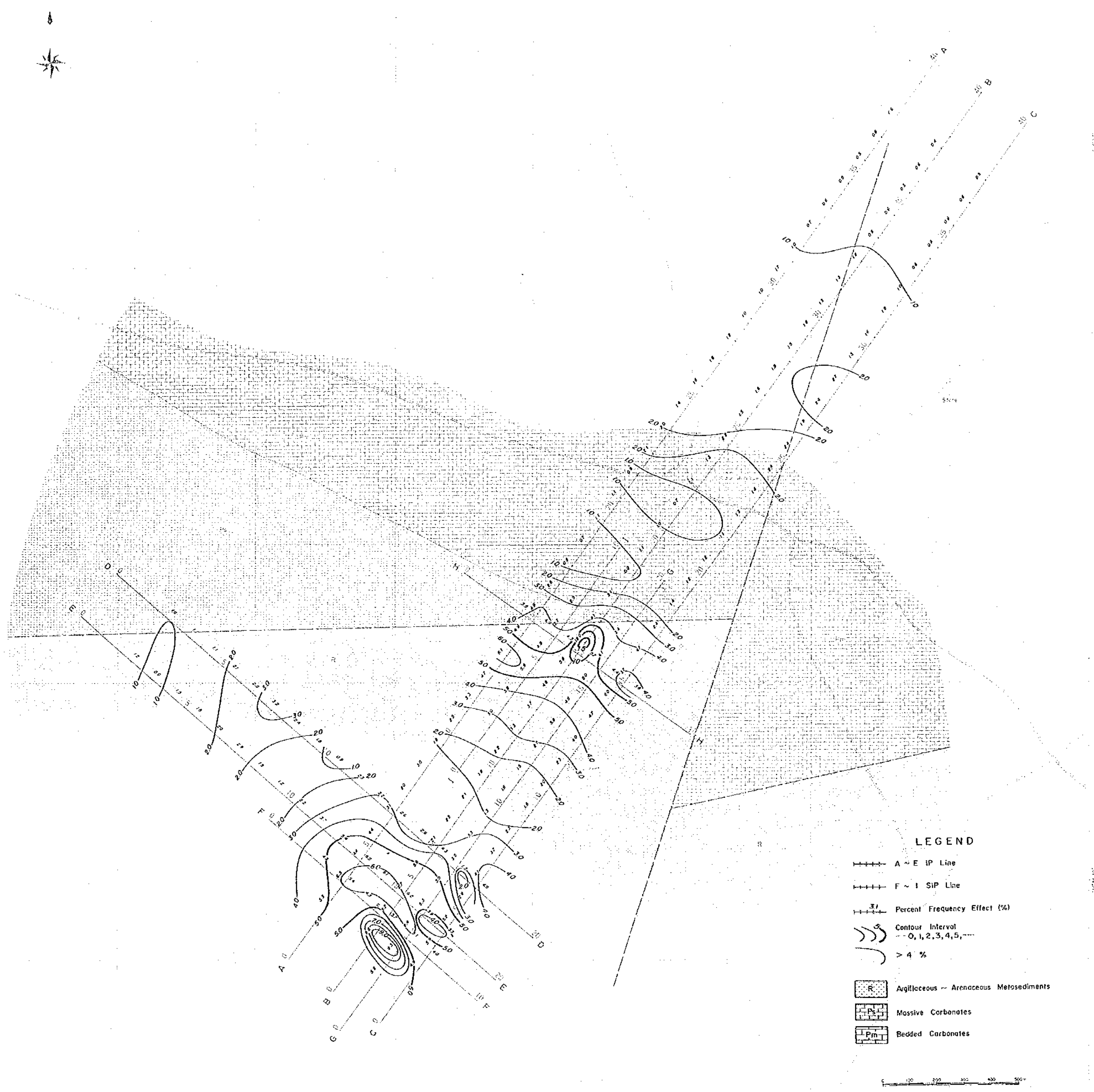

Fig. 24 Plan Map of Percent Frequency Effect [N=3]

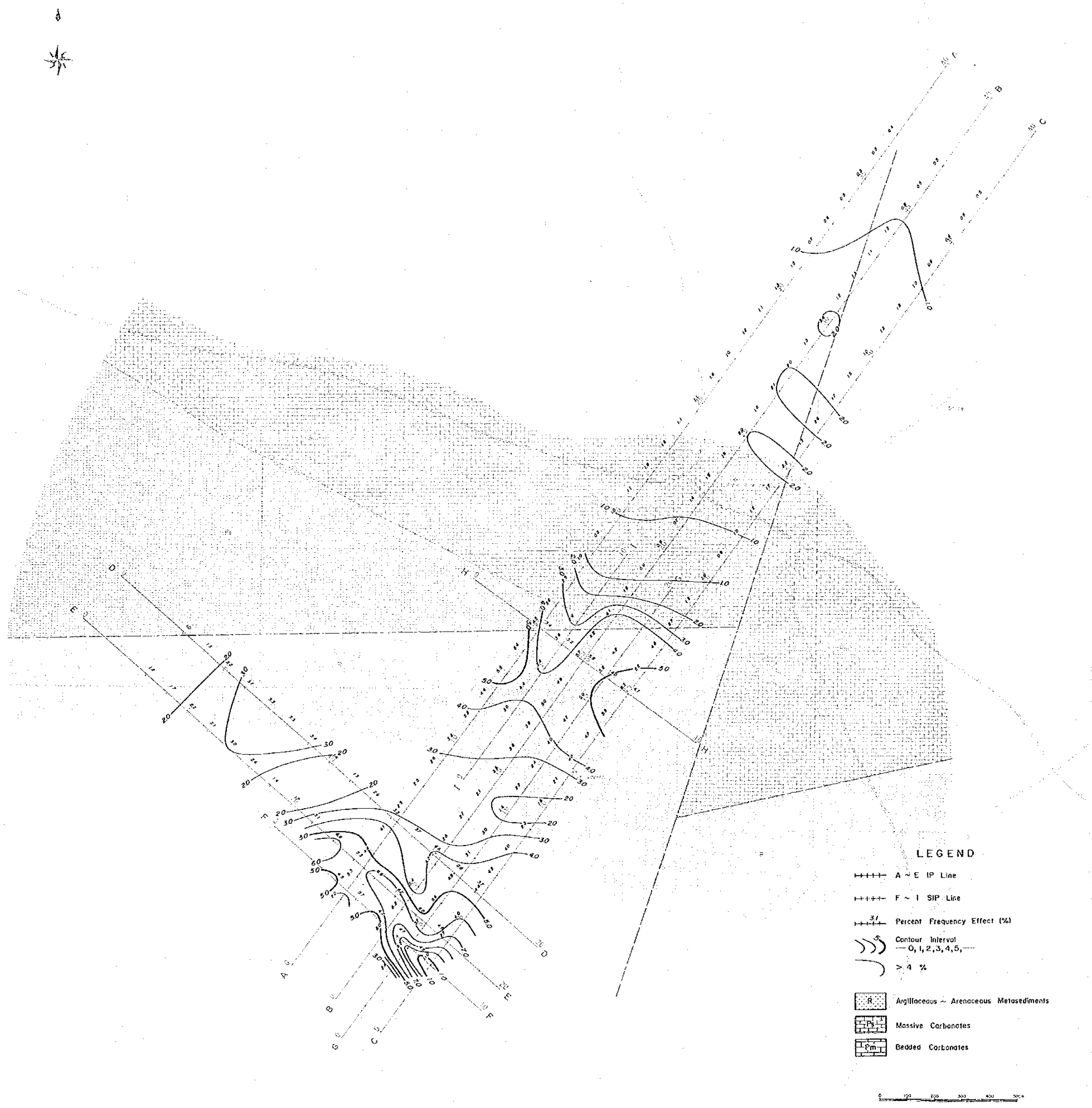

Fig. 25 Plan Map of Percent Frequency Effect [N=4]

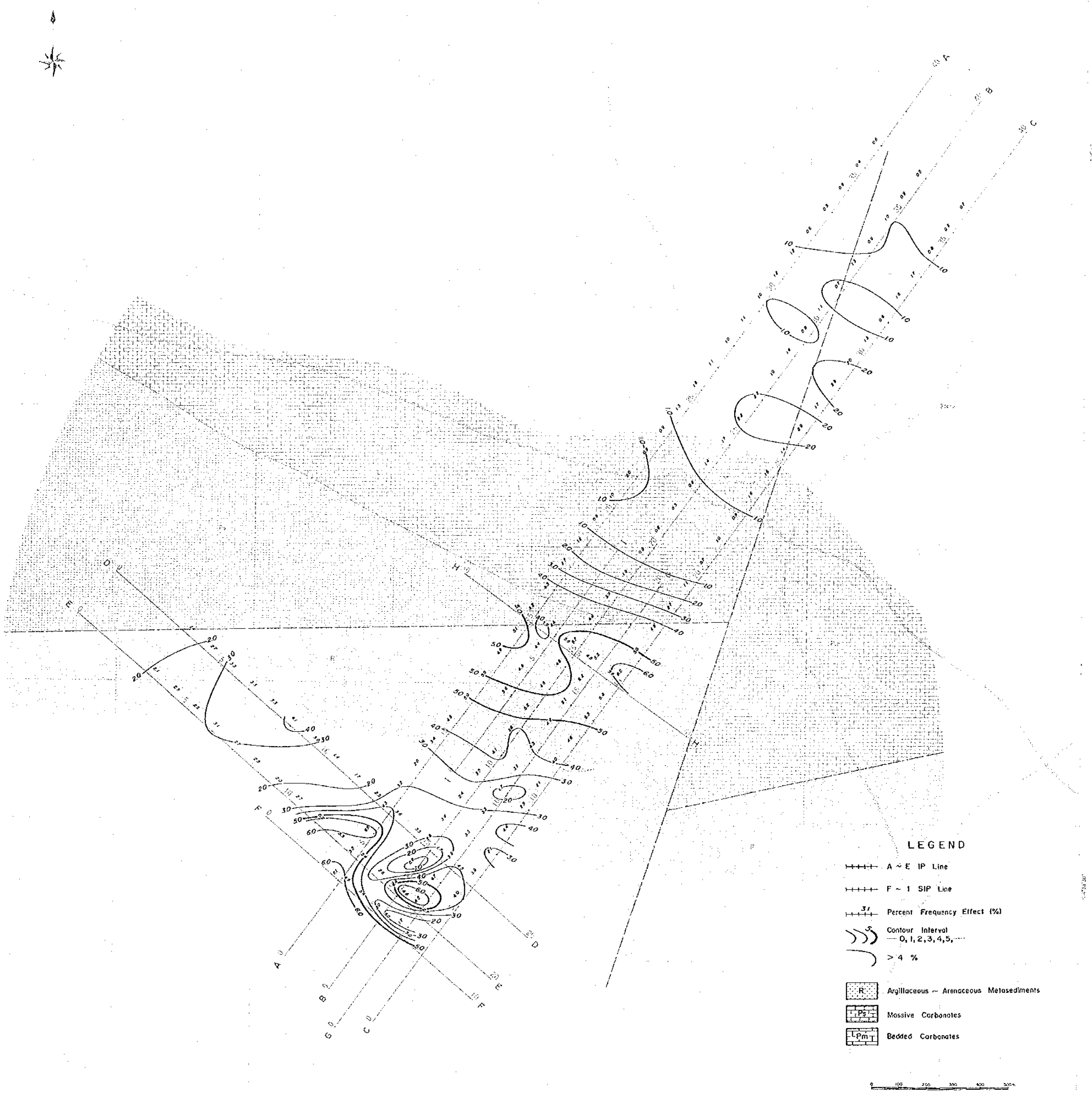

Fig. 26 Plan Map of Percent Frequency Effect [N=5]

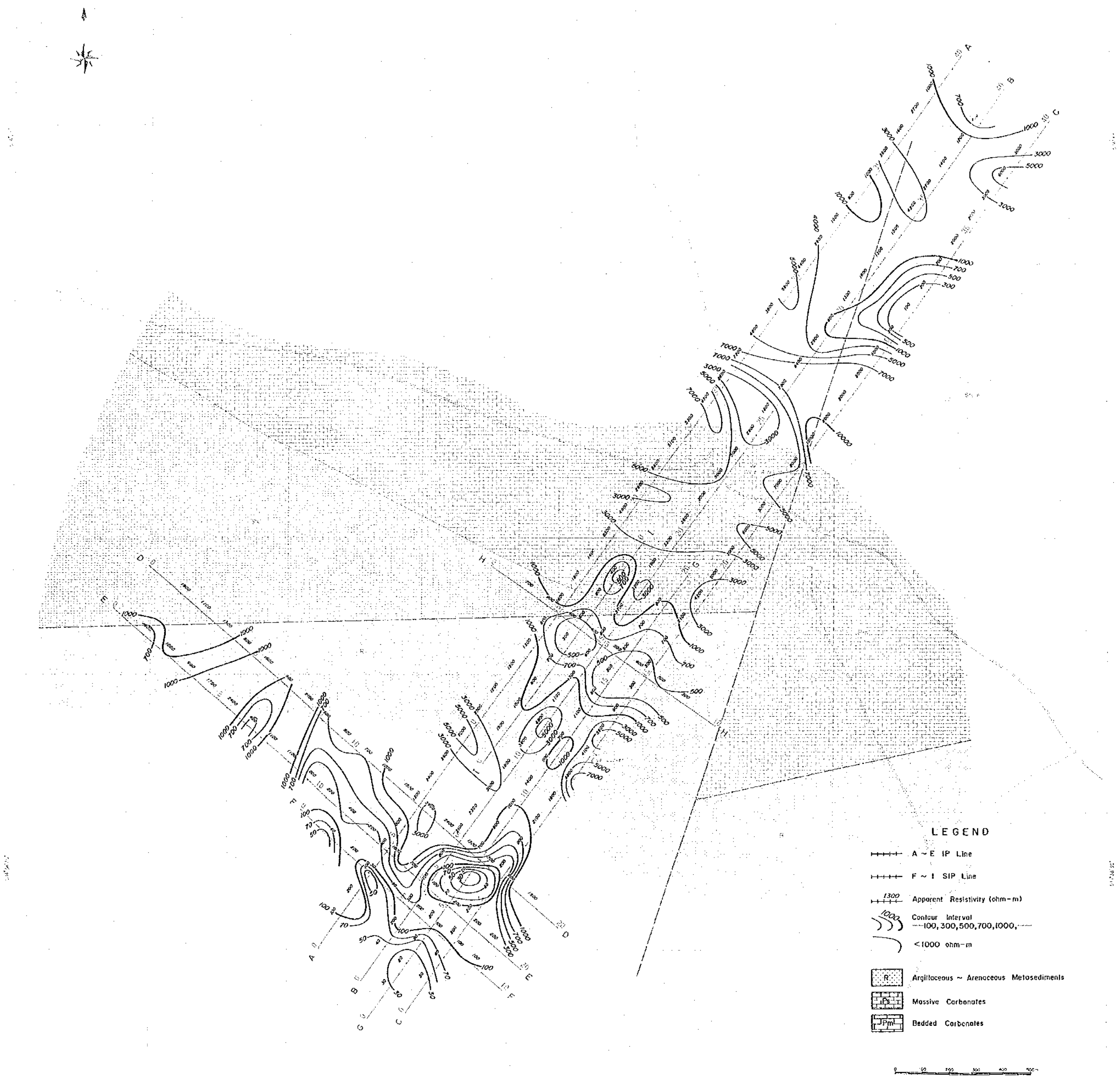

Fig. 27 Plan Map of Apparent Resistivity [N=1]

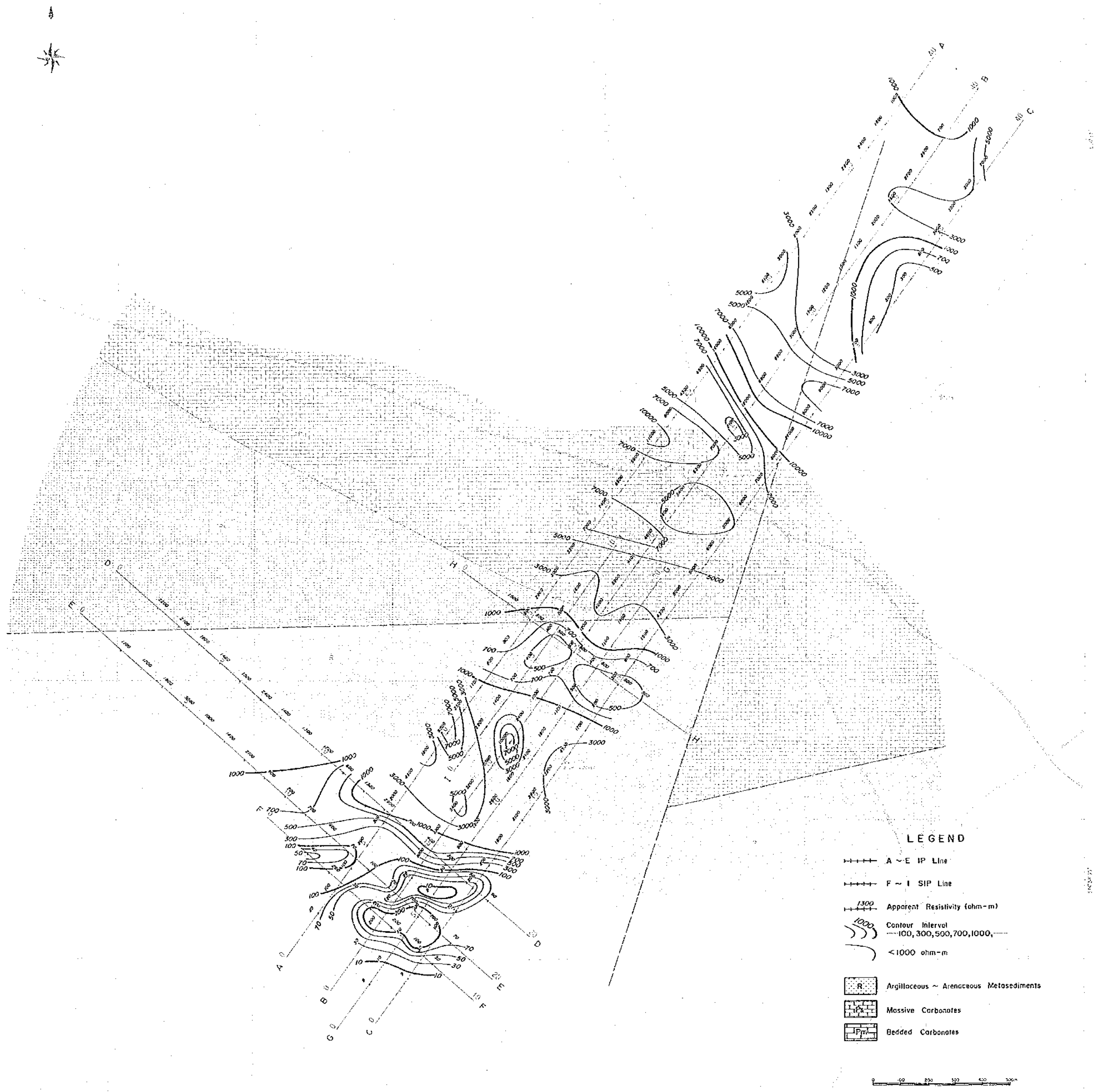

Fig. 28 Plan Map of Apparent Resistivity [N=2]

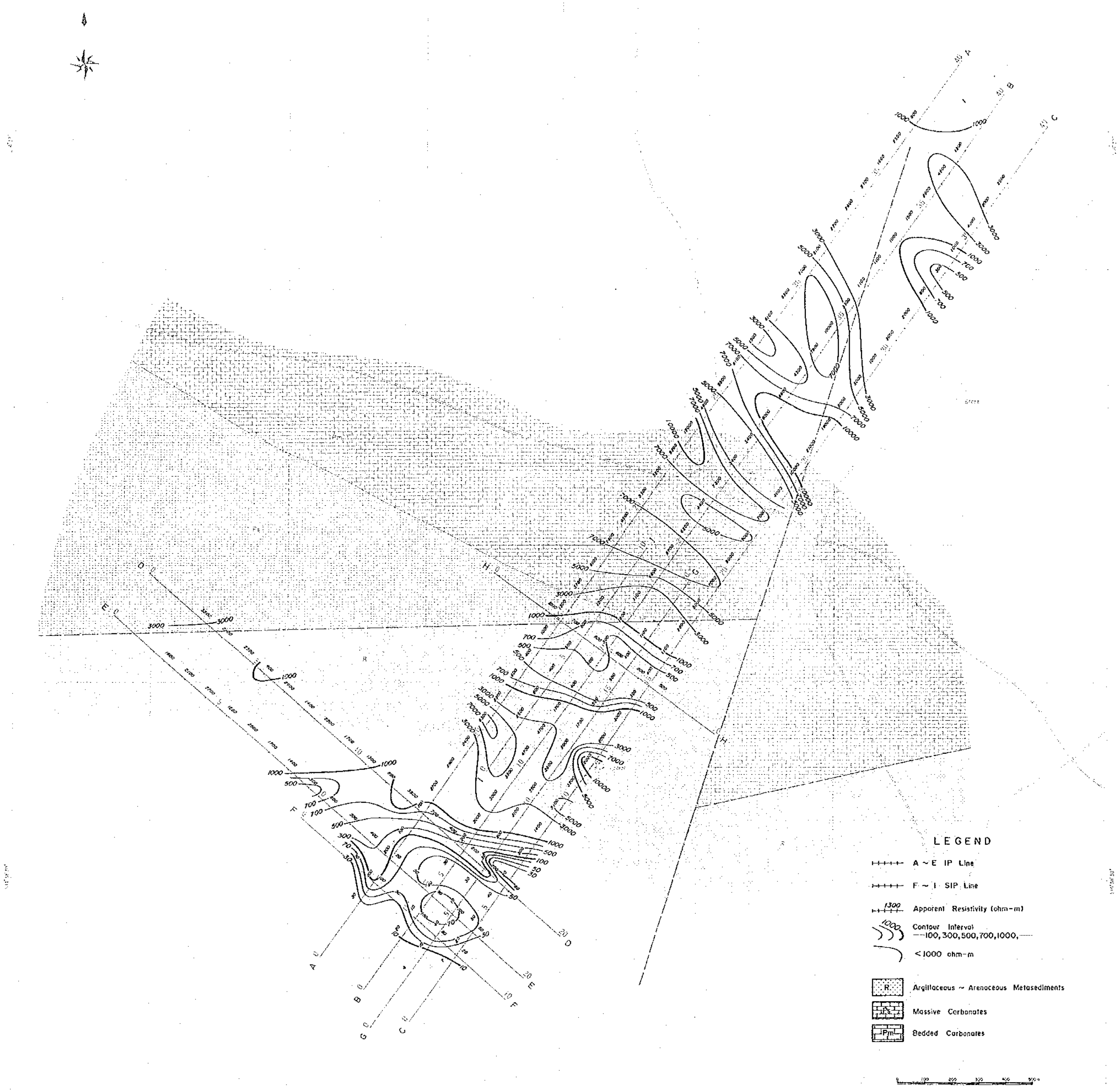

Fig. 29 Plan Map of Apparent Resistivity [N=3]

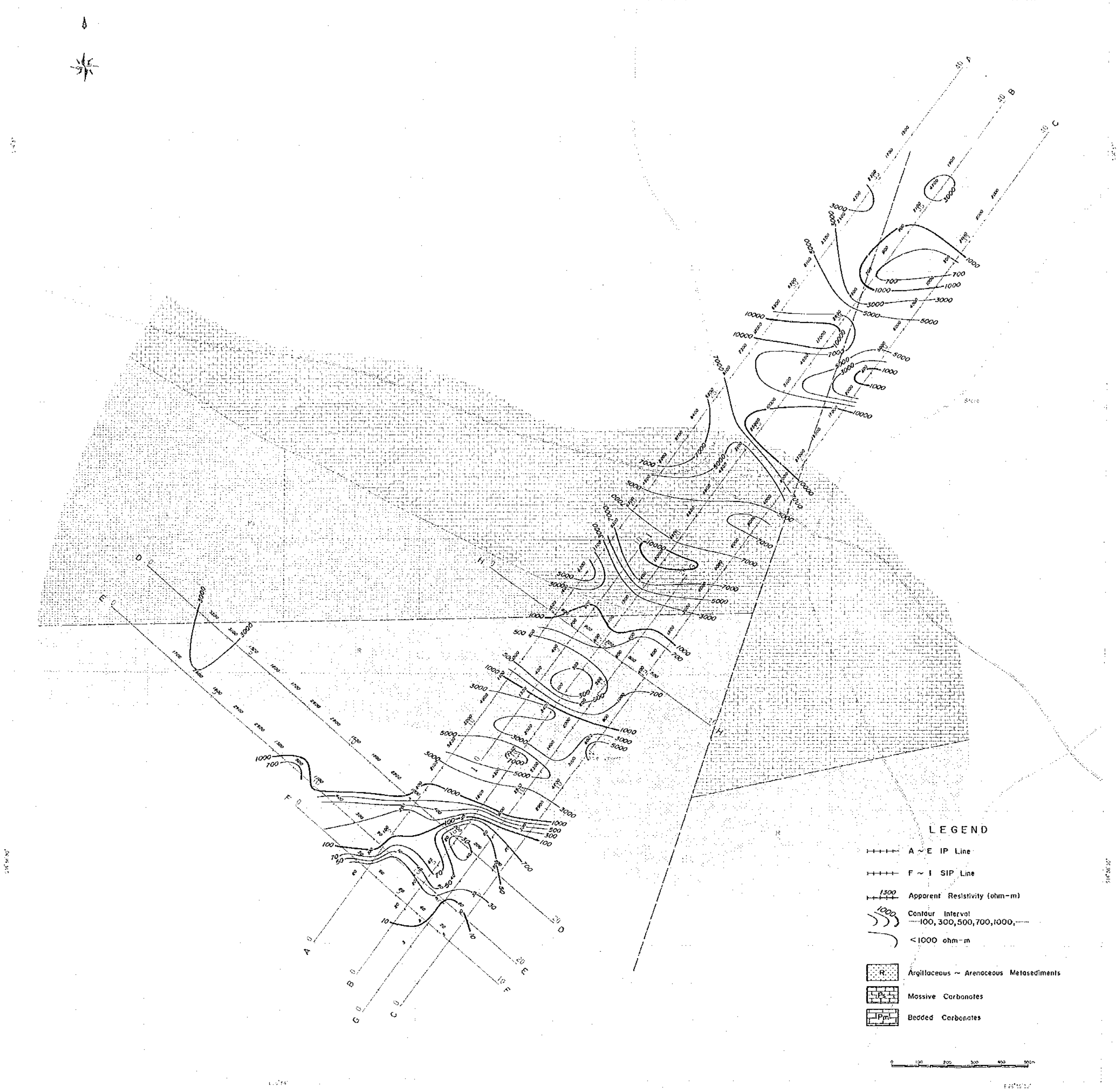

Fig. 30 Plan Map of Apparent Resistivity [N=4]

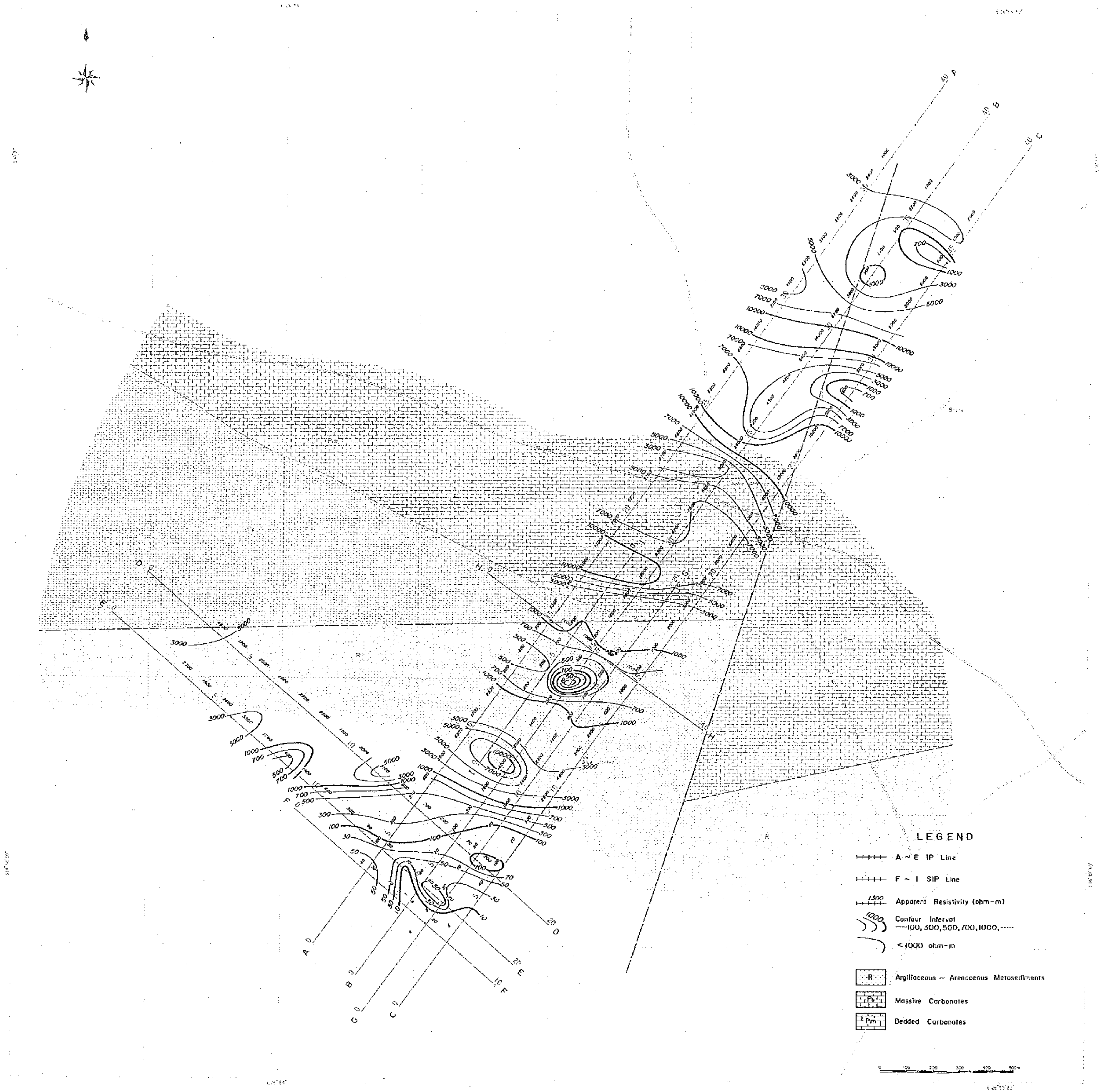

Fig. 31 Plan Map of Apparent Resistivity [N=5]

The anomaly zone No.4 is confined by a contour of 4% at the intersections of lines A,B,C and G with lines D,E and F. The data of resistivity indicated the existence of a tectonic line which trended in an east-west direction. The position of this tectonic line approximately coincides with that of a contour line of 100 ohm-m in apparent resistivity which passes by the vicinity of intersections of line A with F and of line G with D on a plan of apparent resistivity at n=2 (Fig. 28).

The zone of low resistivity on the southern side of a contour line of 100 ohm-m is accompanied by PFE anomalies which can be separated into two parts, one being an anomaly along the tectonic line and another being an anomaly in the zone of low resistivity of less than 10 ohm-m at the southern end of the area.

(2) Contours PFE, n=4 (Fig. 25)

The anomaly zone No.5 is defined by a contour of 3% which encloses an area of stations 6 to 9 on line D and station 7 on line E. The zone becomes obvious from the contours at n=4 indicating a depth of some 250m. The anomaly zone is considered to be in limestones due to high resistivities ranging from 1,000 to 3,000 ohm-m.

(3) Contours of AR, n=2 (Fig. 28)

A supplemental explanation is added to the zones of PFE anomalies from Nos. 1 to 4 from the point of view of apparent resistivity.

The anomaly zone No. 1 around stations 28 on line B and 28 on line C has an apparent resistivity ranging from 5,000 to 7,000 ohm-m and is situated within or in the vicinity of a zone of high resistivity. It may be possible to indicate a mineralized zone associated with silicification in limestone beds.

The anomaly zone No.3 will be reviewed later on with a result of similation.

The anomaly zone No.4 can be separated into northern and southern parts by the existence of a closed contour of 100 ohm-m in the middle which corresponds to a limestone hill.

(4) Contours of AR, n=4 (Fig. 30)

The anomaly zone No.5 around stations 6 to 9 on line D and at station 7 on line E has an apparent resistivity ranging from 1,000 to 3,000 ohm-m but does not give a distinct pattern. It can be assumed that the electromagnetic coupling has not been encountered in data because of being highly resistive, and there remains a possibility that a mineralized zone exists in a depth of some 250m.

3-3 Raw Phase Section

To find the SIP characteristics of the anomaly zones Nos. 3 and 4, the raw phase sections were provided at frequencies of 0.125, 0.375, 0.625, 1.0 and 3.0 Hz (Fig. 32, Fig. 33).

(1) Raw Phase Sections of Zone No.3

Three SIP lines, G, H and I, went across the anomaly zone No.3. The raw phase sections (Fig. 32, Fig. 33) of each line are very similar to the pseudosections of PFE. The most similarity is observed on the raw phase section at a frequency of 0.125Hz. A 4 to 5%PFE anomaly is correlative with a raw phase of -30 to -40 m rad. When a frequency increases (i.e., 0.125 to 3 Hz), a raw phase remains unchanged or slightly decreases its absolute values, and on the contrary, the absolute value of raw phase in background increases. Consequently, the raw phase characteristic of the anomaly zone becomes similar to that of ore sample and the characteristic of background seems similar to that of limestones.

(2) Raw Phase Section of Zone No.4

SIP lines which intersect the anomaly zone No. 4 are lines F and G. The raw phase section (Fig. 32) gave a pattern of anomaly similar to that of PFE pseudosection in a low frequency range of 0.125 to 0.375 Hz. The strongest resemblance to PFE pseudosection is illustrated in a raw phase section at 0.125 Hz. A PFE of 4 to 5% corresponds to a raw phase of -30 to -40 m rad. A change in raw phase

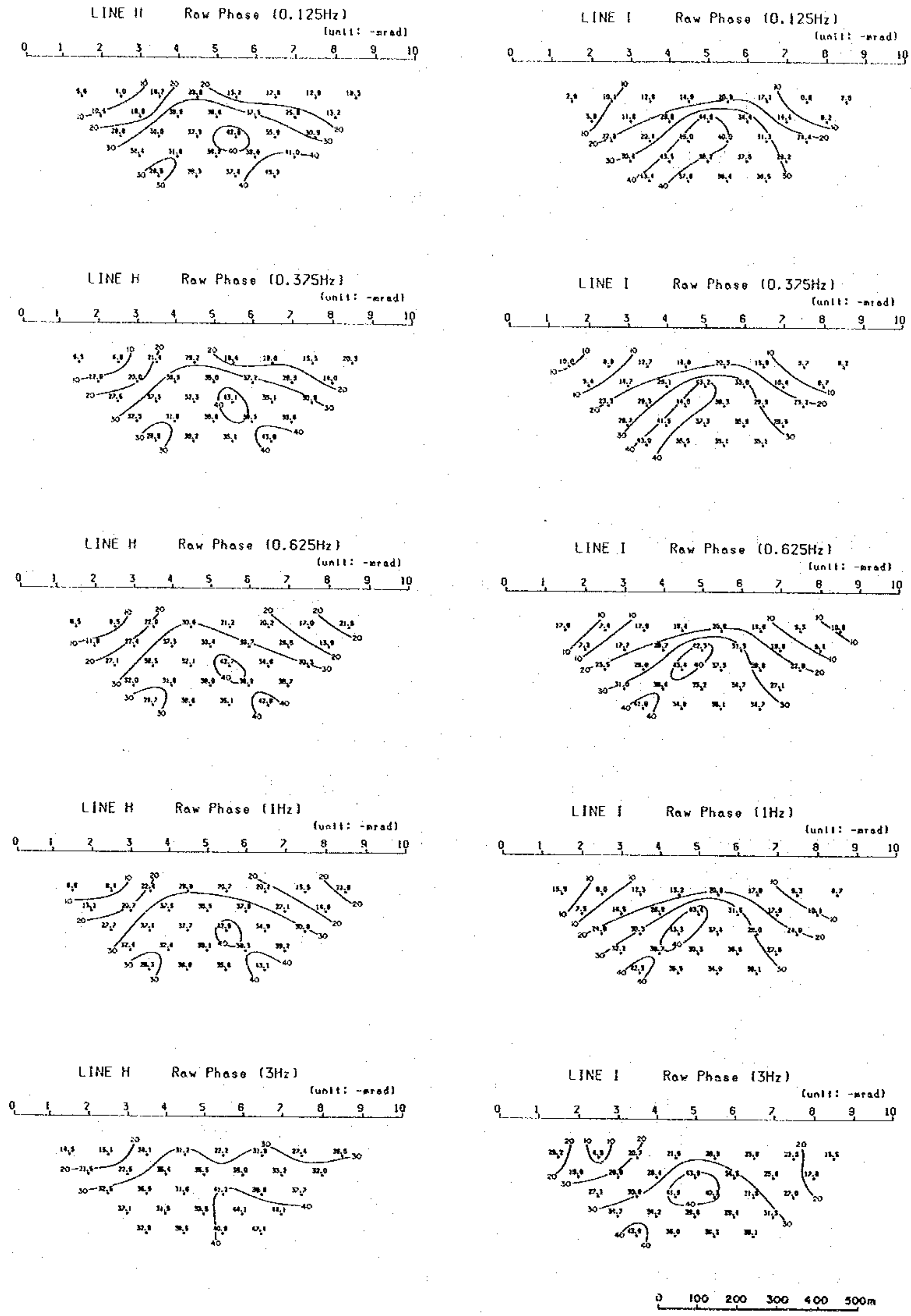

Fig. 33 Raw Phase Section of Lines H, I

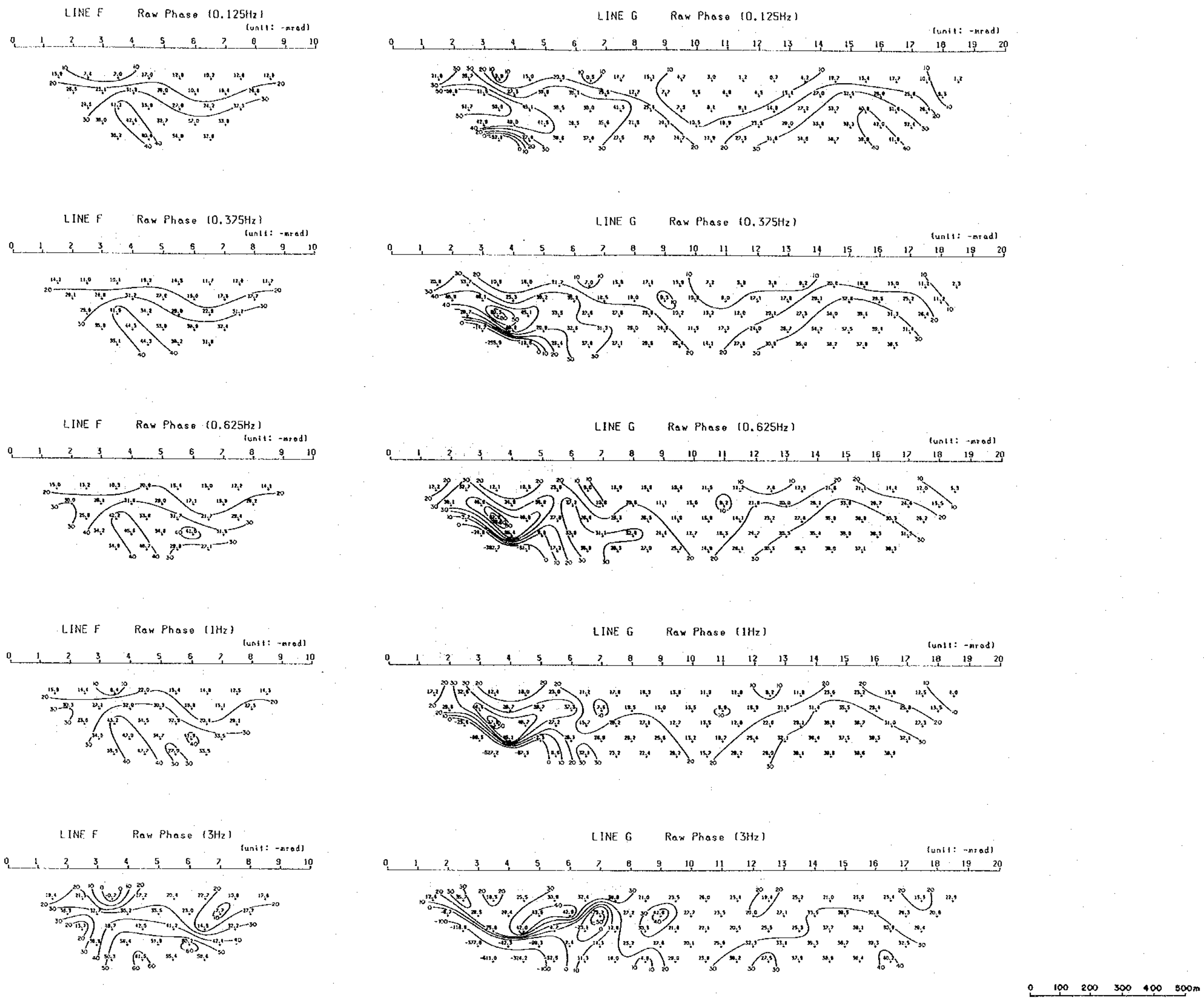

Fig. 32 Raw Phase Section of Lines F, G

in connection with an increase in frequency is obviously different from the case of the anomaly zone No.3. Details of this point is discussed with a phase spectrum in the following section.

3-4 Phase, Magnitude and Cole-Cole Diagrams

Spectral sections consist of Cole-Cole diagram, phase spectrum and magnitude spectrum. The spectral characteristics of the anomaly zones Nos. 3 and 4 are discussed below.

(1) Spectral Characteristic of Zone No.3

Anomalous zones are located between stations 14 and 16 on line G(Fig. 34), 4 and 6 on line H, and 4 and 6 on line I (Fig. 35).

The phase in the anomaly zone No.3 ranges from -30 to -40 m rad and shows a stable to slightly decreasing spectrum with an increase of frequency in a low region of 0.125 to 3.0 Hz but increases in a high region of 3 to 88Hz. The phase spectrum has been strongly affected by an electro magnetic coupling in a region of high frequencies. Positive phases are seen between stations 12 and 13 on line G at n=5 (Fig. 34) and at station 4 on line I at n=4.

Almost magnitudes decrease as a frequency increases but an increase of magnitude in a high range of frequencies is observed between stations 12 and 13 on line G at n=5.

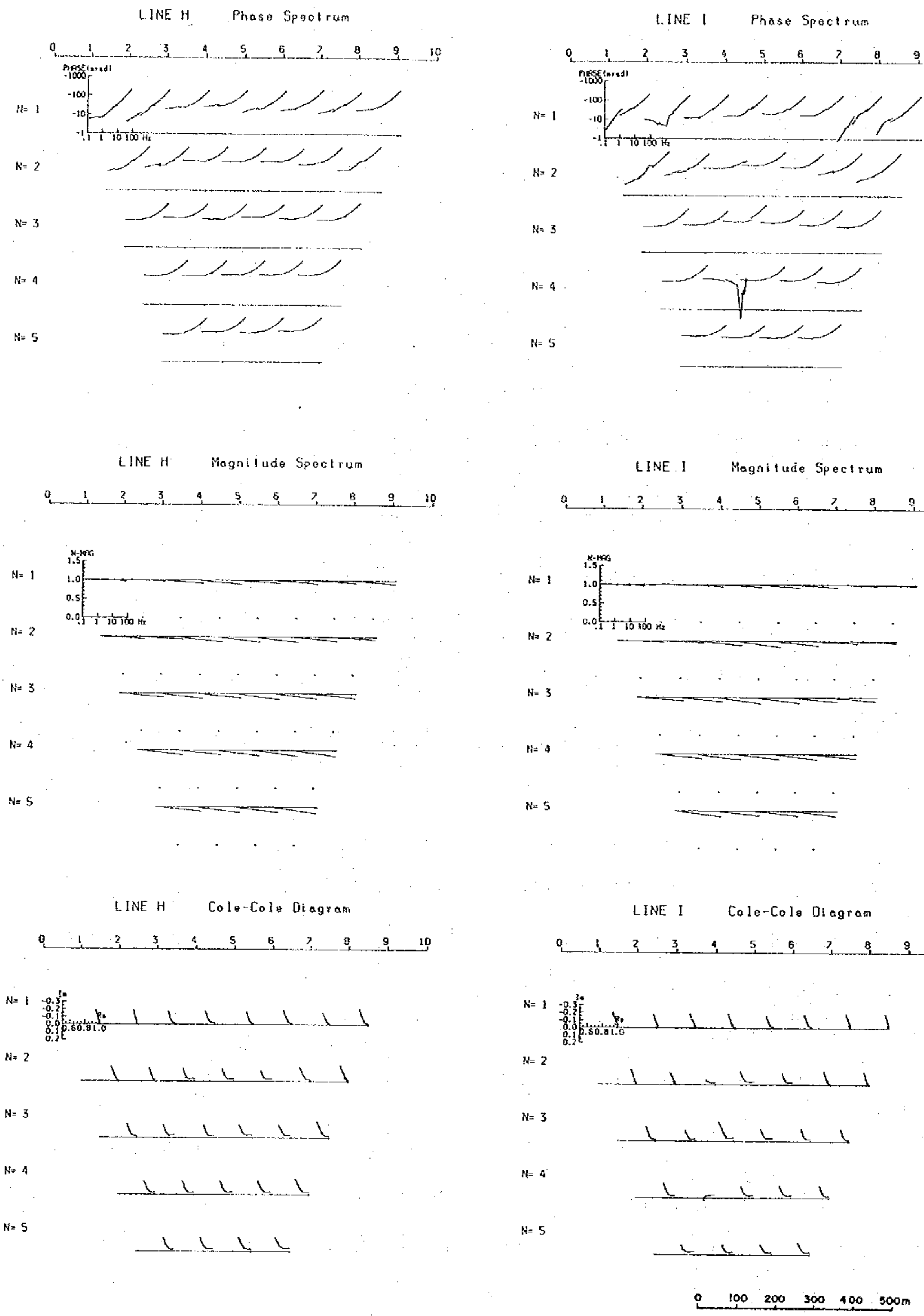

Fig. 35 Phase, Magnitude, Cole-Cole Section of Lines H, I

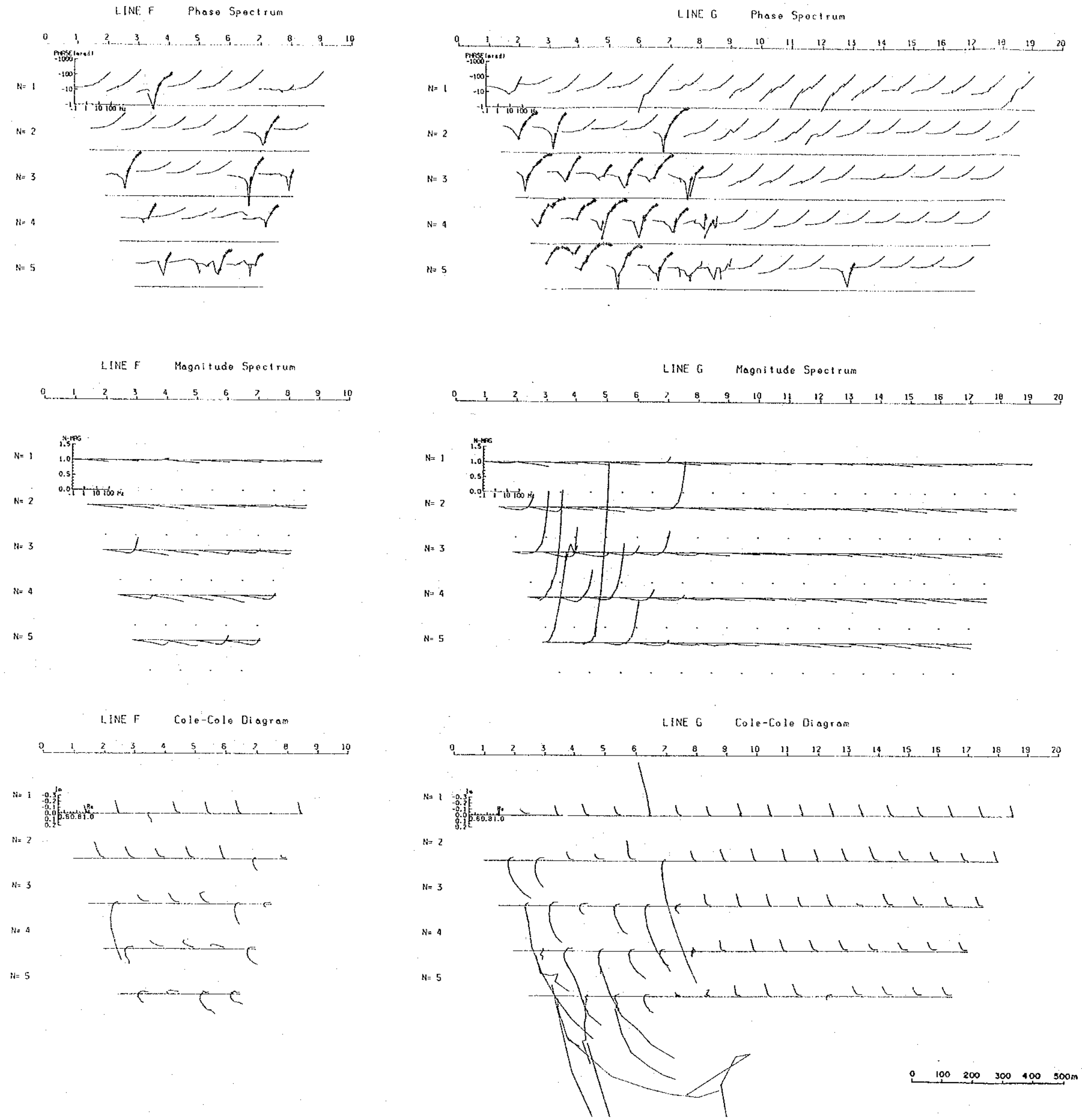

Fig. 34 Phase, Magnitude, Cole-Cole Section of Lines F, G

Cole-Cole Diagrams are generally of patterns of left-hand-side-up, but some special patterns are noticeable between stations 13 and 14 at n=3, 12 and 13 at n=5 on line G, and at station 4 at n=4 and between stations 4 and 5 at n=3 on line I.

These positive phases in a high frequency region, increases of magnitudes and special patterns of Cole-Cole diagrams are found in the vicinity of boundaries of a zone of high resistivity with a zone of low resistivity, indicating an origin due to the existence of a border where a value of resistivity sharply changes.

(2) Spectral Characteristic of Zone No.4

The anomaly zone refers to a section between stations 3 and 8 on line F, and 2 and 7 on line G (Fig. 34). There can be seen two patterns of phase characteristics. One is a normal pattern in which a phase value of -30 to -40 m rad at 0.125 Hz increases in association with frequency. Another pattern is of that a phase is rather uniform or on a slight decrease in a low region of frequency at 0.125 to 3 Hz and that in a higher frequency range a phase becomes of a positive large values, an increase of magnitude and a large positive imaginary number component in the Cole-Cole diagram have been obtained.

These phenomena were recorded where a sharp change of resistivity was observed due to an existence of a bed of extremely low resistivity.

3-5 Spectral Sections after Decoupling

As already stated, Hallof and Pelton divided the electromagnetic coupling into two groups, one being of a uniform earth, the other being of a conductor. The coupling caused by a uniform earth (normal coupling) is represented by an increase of negative phase value and a decrease of magnitude when a frequency is increased. On the other hand, the coupling effect caused by a conductor is expressed by increases of both positive phase value and magnitude as a frequency increases. This sort of coupling is often observed where a resistivity abruptly changes laterally or vertically due to an existence of a zone of low resistivity.

The electromagnetic couplings in lines which traverse the anomaly zone No.3 are usually of normal, but coupling effects in conductors are seen between stations 12 and 13 on line G at n=5 (Fig. 34) and at station 4 on line I at n=4 (Fig. 35). No coupling effect of this sort is found on line H (Fig. 35), probably the line being along a zone of low resistivity, namely, the anomaly zone No.3.

The electromagnetic coupling consists not only of normal but also of strong coupling in a conductor. This may be explained by a sharp change in resistivity from several 1,000s to less than 10 ohm-m in the vicinity of station 7 on line G (Fig. 21).

The results of decoupling are illustrated in various spectra (Fig. 36), PFE pseudosections (Fig. 37) and phase

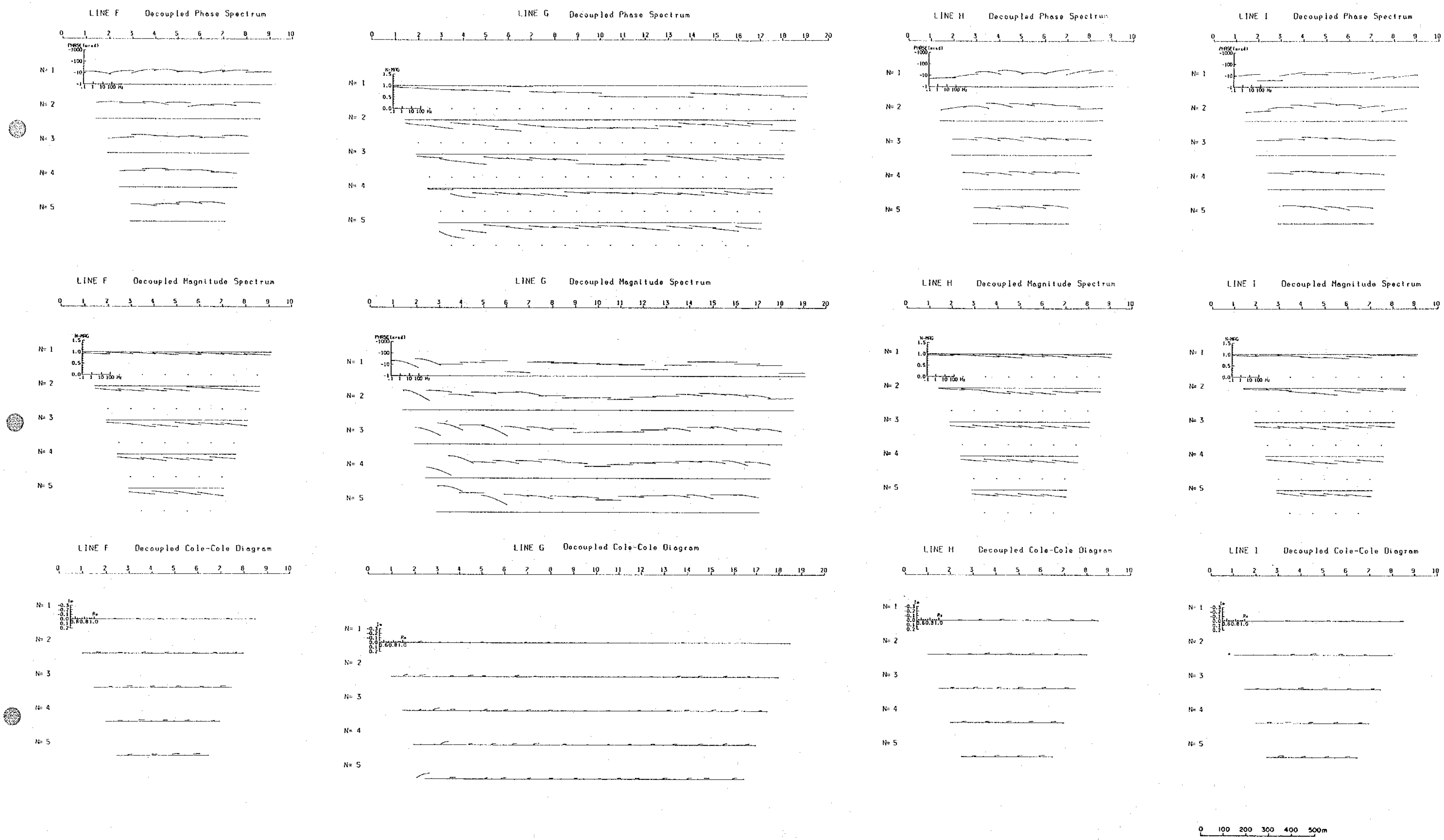

Fig. 36 Decoupled Phase, Magnitude, Cole-Cole Section of Lines F, G, H, I
Section of Lines F, G, H, I

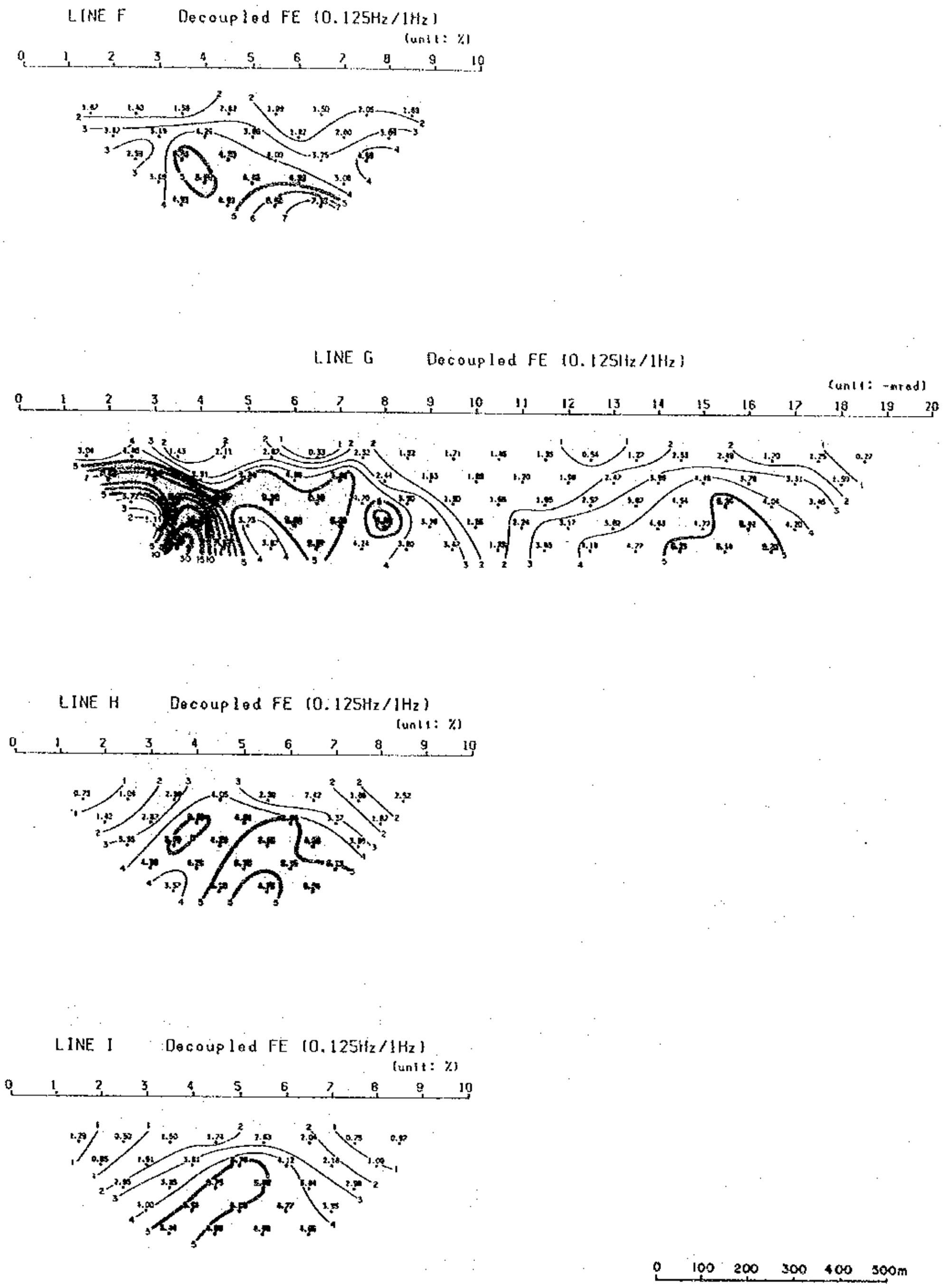

Fig. 37 Decoupled Percent Frequency Effect of Lines F, G, H, I

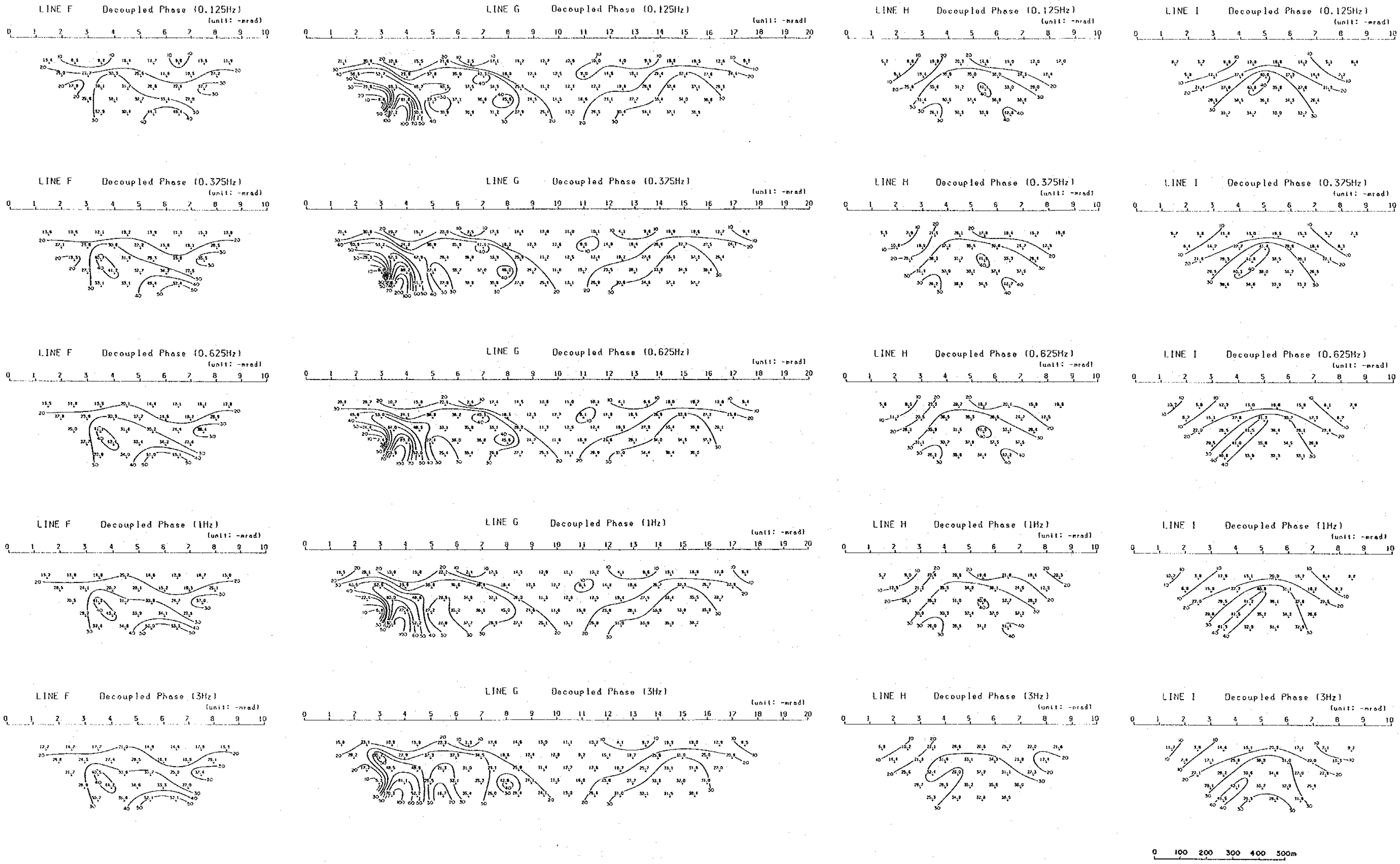

Fig. 38 Decoupled Phase Section of Lines F, G, H, I

sections (Fig. 38) after removals of coupling effects.

No essential changes of patterns or values in PFE pseudosections and raw phase sections (Figs. 37, 38) of anomaly zone No. 3 are not observed on lines G,H and I.

In the profiles of anomaly zone No.4 over lines F and G, positive raw phases have vanished and PFE values have increases in some stations. Nevertheless, decoupling on anomaly zone No. 4 cannot be deemed to be enough due to poor quality of data (owing to low signal to noise ratio in a low resistive area) and due to strong coupling effects caused by a conductor.

3-6 Simulation

Simulation is conducted to delineate a shape, a depth and resistivity of zone No.3 which showed a comparatively coherent pattern of anomaly.

The anomaly zone No.3 gives similar patterns on apparent resistivity and frequency effects over traverse lines A,B,C,G and I (Figs. 19 ∿ 21), indicating that the zone extends in a direction of WNW-ESE which intersects these lines.

AR pseudosections show that, in the western half of the anomaly on lines A, I, and B, the anomaly zone dips slightly to the south, and that, in the eastern half on lines G and C, the zone dips vertically.

A high value of PFE occurs in a shallow depth from 100 to 150 m on line A. On the other hand, a high value appears in a deep from 200 to 300 m on line C. From these, the anomaly zone seems to be shallow in the west and deep in the east.

A typical result of simulation is shown in Fig. 39. The result shows that resistivity of the anomaly zone can be deemed of the order of 100 ohm-m, similar to an average resistivity of ore samples (Table 4). The width of a zone of low resistivity is estimated to be of some 200 m and within this zone, a zone of high frequency effects is placed being of 60 to 70 m in width. This model gives an image of mineralized zone in sediments adjoined to limestones. A depth of the top of the zone is assumed to be about 100 m.

3-7 Interpretation of Geophysical Anomalies

Five zones of geophysical anomalies from Nos. 1 to 5 have been delineated as illustrated in Fig. 40. The characteristics of each zones are as follows.

(1) The zones Nos. 1 and 2 are situated in limestones and extended in WNW to ESE directions, especially the zone No. 2 passing across Sable Antelope old workings. These anomalies have high resistivities ranging from 5,000 to 10,000 ohm-m and are assumed to be of mineralized zones associated with silicification. The depths of tops of mineralized zones would be less than 100 m.

(2) The zone No.3 lies in metasediments surrounded by limestones or in the vicinity of a boundary of these rocks and extends in a WNW-ESE direction. Blue Jacket mineralization is known 300m south of this zone. From a result of simulation, the anomaly zone is estimated to be of low resistivity of some 100 ohm-m in a background of several thousand ohm-m. The value of estimated resistivity and a phase spectrum observed are of similar physical properties of ore samples. An existence of mineralized zone can be expected with a top of about 100m deep.

(3) The zone No.4 in metasediments consists of two anomalies, one being along a tectonic line of an east-west direction, the other being at a southern end. These anomalies are situated within a broad zone of low resistivity where electromagnetic coupling are often encountered. A strong electromagnetic coupling is observed in the anomaly at the south end. Therefore, a preference is given to the anomaly along the tectonic line.

(4) The zone No.5 is situated in the vicinity of a boundary between limestones and metasediments, but probably in limestones because of high resistivity. The depth of it is estimated more than 200m.

MODEL NO C

CODE	RESISTIVITY OHM M	F.E. %
1	600.	1.0
2	100.	.0
3	4000.	.0
4	100.	25.0
5	0.	.0
6	0.	.0
7	0.	.0
8	0.	.0
9	0.	.0

Simulation Model

Depth	Row	10	11	12	13	14	15	16	17	18	19
	1	111	111	111	111	111	111	111	111	111	111
	2	333	333	333	333	111	111	333	333	333	333
	3	333	333	333	333	111	111	333	333	333	333
-100m	4	333	333	333	333	224	422	333	333	333	333
	5	333	333	333	333	224	422	333	333	333	333
-200m	6	333	333	333	333	224	422	333	333	333	333
	7	333	333	333	333	224	422	333	333	333	333
	8	333	333	333	333	224	422	333	333	333	333
-300m	9	333	333	333	333	224	422	333	333	333	333
	10	333	333	333	333	224	422	333	333	333	333
	11	333	333	333	333	224	422	333	333	333	333
	12	333	333	333	333	224	422	333	333	333	333
	13	333	333	333	333	224	422	333	333	333	333
	14	333	333	333	333	224	422	333	333	333	333

Pseudo-Section of Line C

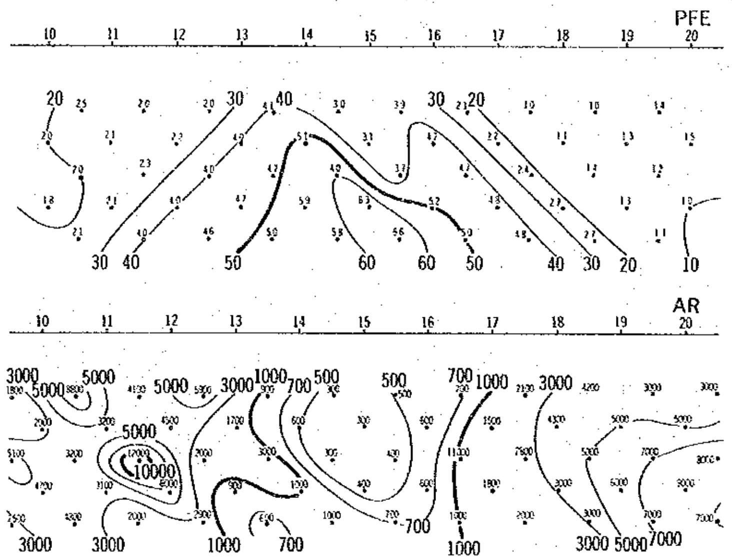

Calculated Anomaly

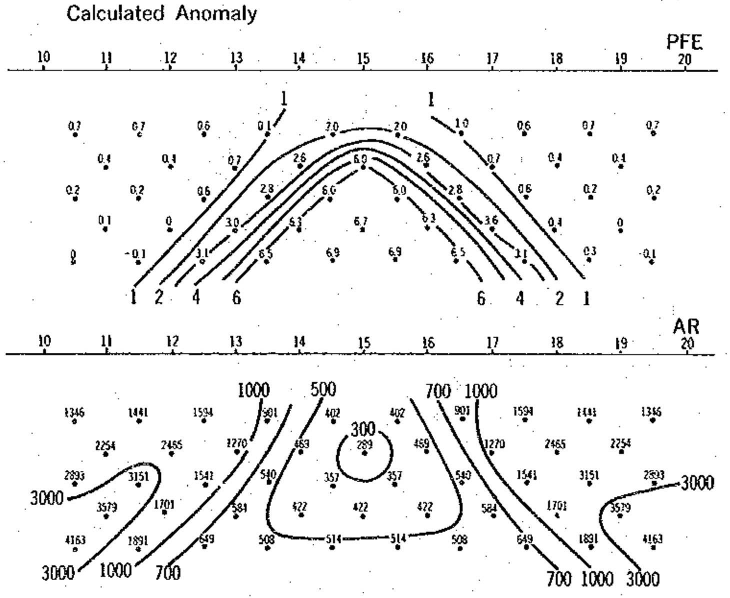

Fig. 39 Simulation Model

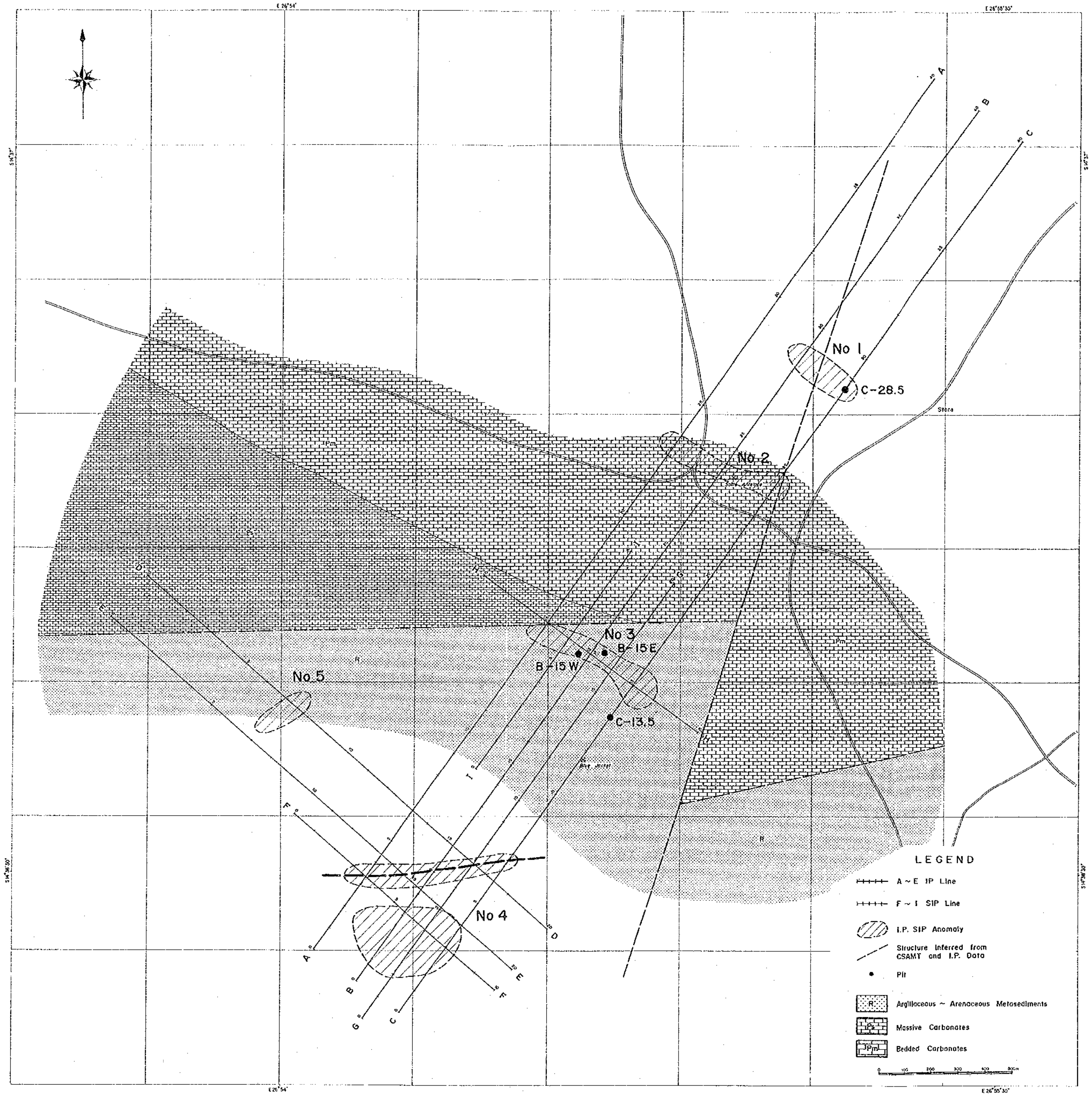

Fig. 40 IP, SIP Interpretation Map